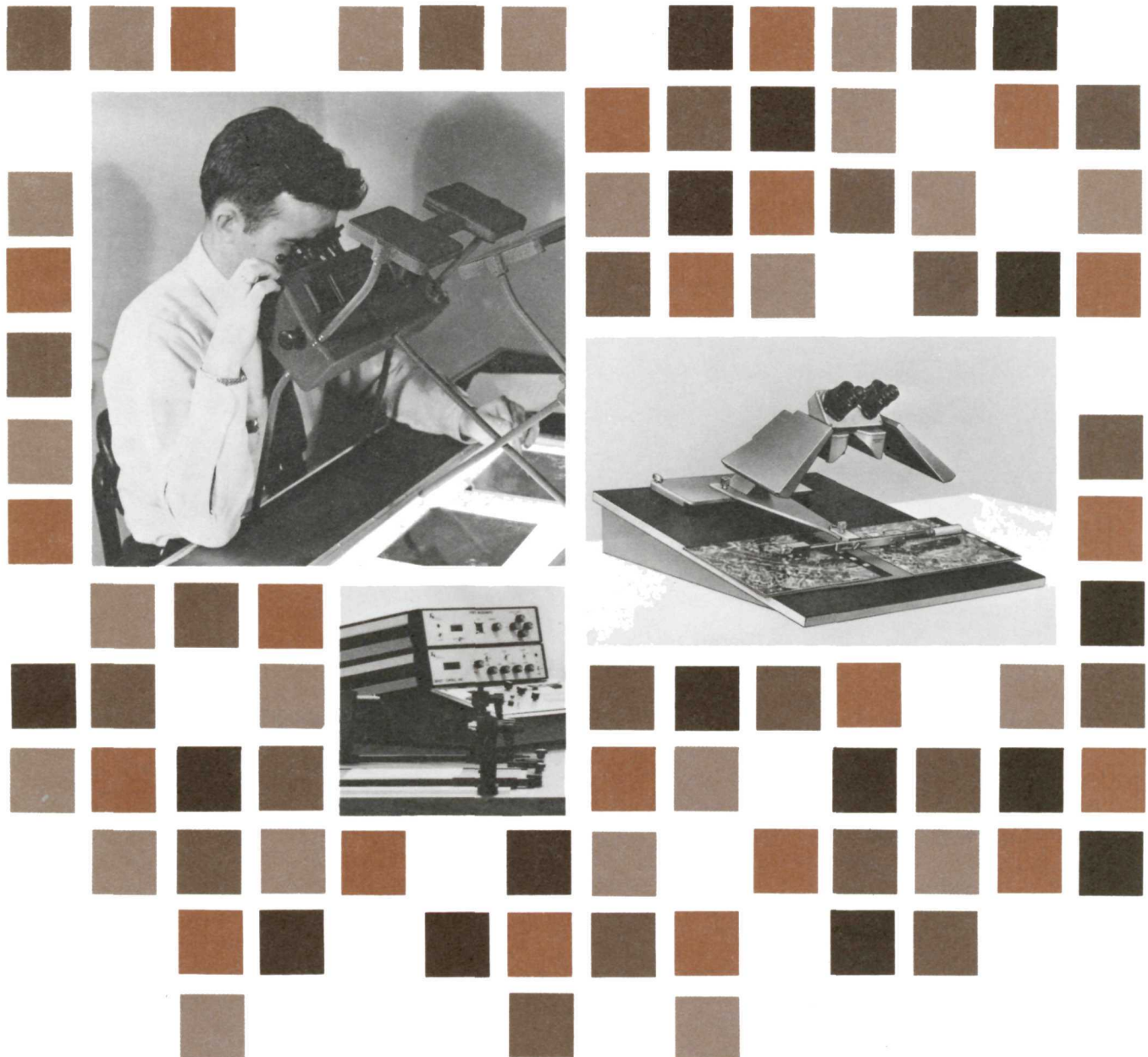


REMOTE SENSING

Instrumentation for
Nondestructive Exploration
of Cultural Resources



REMOTE SENSING

Instrumentation for Nondestructive Exploration of Cultural Resources

**Stanley A. Morain
Thomas K. Budge**

Supplement No. 2

to Remote Sensing: A Handbook for Archeologists and Cultural Resource Managers

Series Editor: Thomas R. Lyons

**Cultural Resources Management
National Park Service
U.S. Department of the Interior
Washington, D.C.
1978**

Library of Congress Cataloging in Publication Data

Morain, Stanley A.

Remote sensing: instrumentation for nondestructive exploration of cultural resources

Bibliography: p.

1. Archaeology—Remote sensing. I. Budge,
Thomas K., joint author. II. Lyons, Thomas R.
Remote sensing. III. Title.
CC76.4.L96 Suppl 2 930'.1'028 78-1417

Cooperating Organizations

National Park Service:

Cultural Resources Management Division, Washington Office
Remote Sensing Division, Southwest Cultural Resource Center

University of New Mexico:

Technology Application Center

National Aeronautics & Space Administration:

Technology Utilization Office

For sale by the Superintendent of Documents,
U.S. Government Printing Office.
Washington, D.C. 20402
Stock Number: 024-005-00736-9

Preface

This supplement is designed for use with *Remote Sensing: A Handbook for Archeologists and Cultural Resource Managers*, by Thomas R. Lyons and Thomas Eugene Avery. The handbook may be obtained by writing the Superintendent of Documents, U.S. Government Printing Office, Washington, DC 20402.

Within the next several months, the National Park Service will publish other supplements to the

handbook dealing with regional applications of remote sensing for archeologists and cultural resource managers. The reader may receive notification of these publications as they become available by writing the Superintendent of Documents (address above) and asking to be placed on mailing list N-557.

Contents

Section 1 Introduction 1

| |
|--|
| Electromagnetic Spectrum 1 |
| Regions of the Spectrum 2 |
| Atmospheric Effects on Radiation 2 |
| Scatter 2 |
| Absorption 3 |
| Refraction 4 |
| Reflection 4 |
| Electromagnetic Radiation Considerations in Archeology 4 |
| Sensors 4 |
| Processing 4 |

Section 2 Sensor Review and Applications in Archeology 5

| |
|------------------------------------|
| Ultraviolet 7 |
| Sensor Operation 7 |
| Basic Image Interpretation 8 |
| Applications in Archeology 9 |
| Multispectral Scanners (Landsat) 9 |
| Sensor Operation 9 |
| Basic Image Interpretation 10 |
| Applications in Archeology 11 |
| Thermal Infrared 12 |
| Sensor Operation 12 |
| Basic Image Interpretation 14 |
| Applications in Archeology 15 |
| Active Microwave Sensors 17 |
| Sensor Operation 17 |
| Basic Image Interpretation 19 |
| Applications in Archeology 21 |
| Passive Microwave Sensors 21 |
| Sensor Operation 21 |
| Basic Image Interpretation 22 |
| Applications in Archeology 23 |
| Ground-Based Instrumentation 24 |

Section 3 Image and Data Processing 39

- Analog Processing Techniques 39
 - Color Additive Viewer 40
 - Diazochrome Color Composites 40
 - Closed Circuit Television Systems 40
 - Frequency Transformations 41
- Digital Processing Techniques 44
 - Densitometry 44
 - Digital Data Tapes 45
 - Classification Strategies 46
 - Band Ratioing 48

Appendix Common Conversion Factors Used in Remote Sensing 50

References 52

Illustrations

- 1-1 Electric and magnetic vectors of an electro-magnetic wave 1
- 1-2 The electromagnetic spectrum 2
- 1-3 Model of incoming electromagnetic radiation 3
- 2-1 Examples of imagery from the visible, thermal, and radar portions of the spectrum 6
- 2-2 Schematic of Landsat multispectral scanner 7
- 2-3 Diagram of luminescence emission and the relationships of growth and decay periods 8
- 2-4 A sample of ultraviolet scanner imagery 9
- 2-5 Reproduction of tonal renditions of twelve spectral regions from a multispectral scanner 13
- 2-6 Divisions of the infrared spectrum 15
- 2-7 Wien's Displacement Law 15
- 2-8 Configuration for a typical infrared scanner 15
- 2-9 Three examples of thermal infrared imagery 16
- 2-10 An example of thermal infrared imagery being used to detect soil moisture variations 17
- 2-11 A schematic of the SLAR system 18

- 2-12 K-Band radar images of vegetation 20
- 2-13 Radar imagery of varying terrain features 22
- 2-14 Configuration of a radiometer and factors affecting received radiation 23
- 2-15 Microwave radiometer (MICRAD) image of Coalinga, California and surrounding region 23
- 2-16 Diagram illustrating the effect of soil moisture on brightness temperature 24
- 2-17 Examples of magnetic anomalies caused by buried cultural features 37
- 3-1 Color additive process 39
- 3-2 Color subtractive process 40
- 3-3 Filtering of Fraunhofer Diffraction Patterns (FDP's) 41
- 3-4 Examples of Fraunhofer Diffraction Patterns 42
- 3-5 Three examples of the use of Ronchi Rulings 43
- 3-6 An example of unsupervised computer classification of crop clusters derived from densitometry of a radar image 47

Color Plates

1. Chart demonstrating essential points of Landsat interpretation 25
2. Landsat image of a portion of the Rio Grande Valley of New Mexico 26
3. A color enhanced passive microwave image of arctic sea ice 27
4. Four examples of the diazochrome process on a Landsat image 28-29
5. Closed circuit television techniques 30
6. Digital image output formats 31
7. Demonstration of pixel overlays as aids in precise coordinate location on Landsat images 30
8. An example of scale adjustments using Landsat digital tapes 32-33
9. Examples of Landsat image corrections 35
10. An example of band ratioing of a Landsat image 36

Tables

- 1-1 Spectral regions, sensors and remote sensing platforms 3
- 2-1 Orbital and sensory parameters of Landsat I and II 11
- 2-2 Comparison of multispectral scanners and their significance for seeing vegetation 12
- 2-3 Thermal properties of typical rock materials 14
- 2-4 Radar bands, bandwidths, and frequency ranges 17
- 2-5 Depth of signal penetration in soils (meters) 18

Section 1

Introduction

The conventional color or black-and-white aerial photograph has been a standard tool of the archeologist for many years. In the last several years, however, we have realized that other portions of the electromagnetic spectrum may be of use in archeology. This supplement to *Remote Sensing: A Handbook for Archeologists and Cultural Resource Managers* will describe the current state-of-the-art of remote sensing other than that involving conventional aerial photography. Different sensors, data processing techniques, and interpretation strategies will be explored, both in a general as well as in an archeological sense. The electromagnetic spectrum is the basis of all that follows. It is therefore requisite that we begin our discussion with a brief review of that topic.

Electromagnetic Spectrum

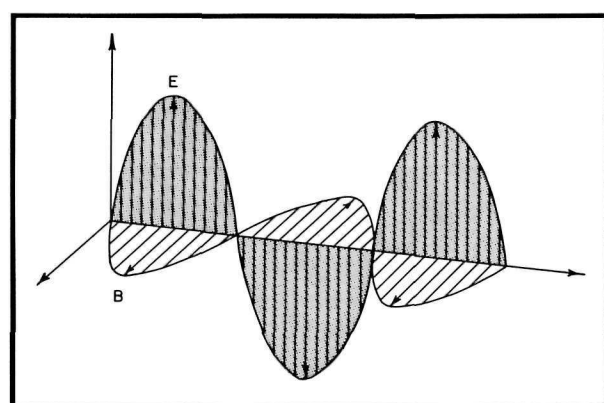
Electromagnetic radiation may be defined as the energy generated by the acceleration of an electric charge. Therefore, any object which has a temperature greater than 0° K will emit electromagnetic radiation of a single or multiple wavelength. The wavelength which is generated is dependent on the length of time over which the acceleration occurs and the frequency on the number of accelerations per second. The particles which are accelerated are electrons, ions and molecules (Nunnally, 1969).

Several theories have been advanced concerning the nature of electromagnetic radiation. One theory is that electromagnetic radiation is propagated in the form of a wave which consists of two fluctuating vectors or fields; one being electric and the other magnetic. The two vectors are perpendicular to the direction of the propagation and are mutually orthogonal as shown in figure 1-1.

The relationship between frequency and wavelength is shown by the formula $\lambda f = c$ or $\lambda = c/f$ where λ = wavelength, f = frequency, and c = speed of light. The formula means that frequency is inversely proportional to wavelength and directly proportional to wave velocity.

A second theory of radiation is that energy is transmitted as discrete units, called quanta, or photons. This theory is based on the idea that the energy of a photon varies directly with frequency and inversely with wavelength—the longer the wavelength, the lower the energy; the shorter the wavelength, the higher the energy. Consequently, in the following discussion, radar has longer wavelengths and lower frequencies than thermal infrared.

At times, electromagnetic radiation behaves as if it were comprised of particles; at other times it reacts like a wave. Neither theory has been totally accepted or rejected.



1-1 Electric (E) and magnetic (B) vectors of an electromagnetic wave. Source: Nunnally, 1969.

Regions of the Spectrum

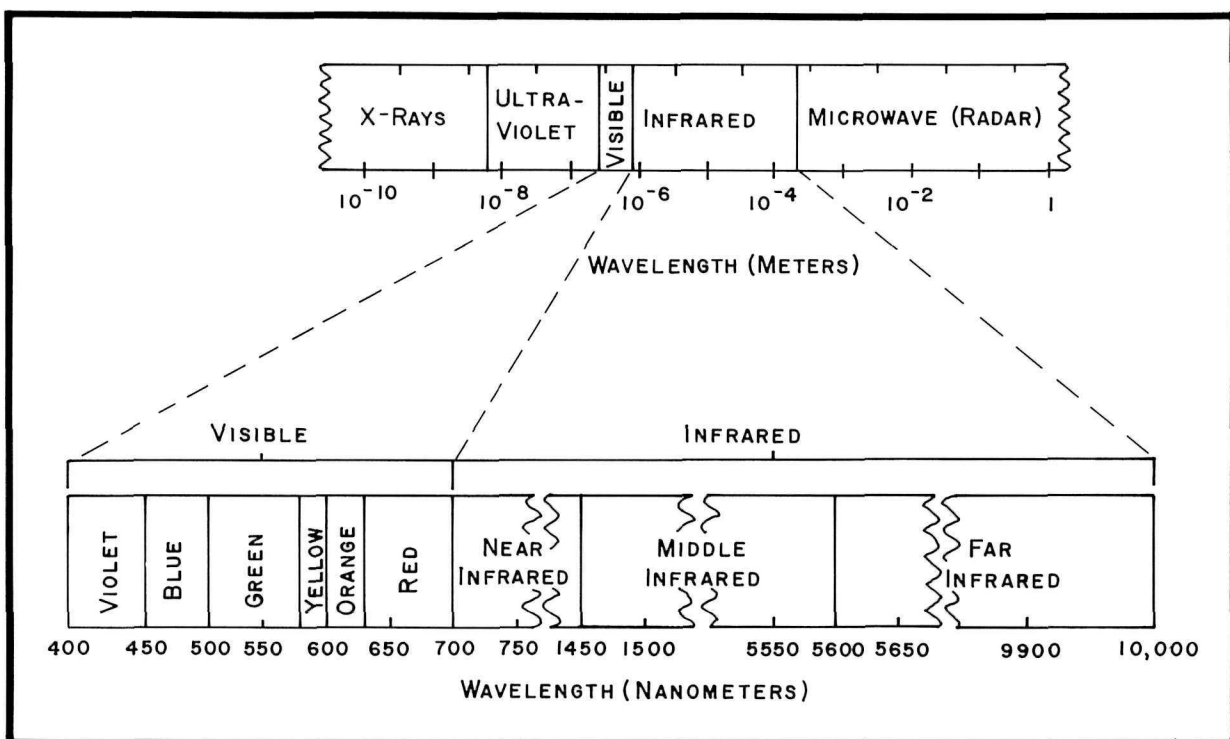
Although the electromagnetic spectrum is a continuum of wavelengths, it has been subdivided into several regions. These regions are cosmic rays, gamma rays, X-rays, ultraviolet, visible, infrared, microwave, radio and acoustic (fig. 1-2). Portions of the spectrum are absorbed by gases such as oxygen and ozone; others suffer scattering due to water and dust particles; and almost all of it is interfered with by other forms of radiometric "noise." Those portions of the atmosphere that are relatively transparent to radiation are called "windows." These are the portions most used in remote sensing of terrain features.

The spectral regions examined in this document are the ultraviolet, visible, reflective infrared (IR), thermal infrared (TIR), passive microwave and radar. The visible and reflective IR regions as sensed through photographic systems have been analyzed in the basic Handbook. Table 1-1 shows the regions of the spectrum, the sensor employed for each region, and the most commonly used platforms.

Atmospheric Effects on Radiation

When electromagnetic radiation moves through a vacuum such as exists above the earth's atmosphere, it moves at the speed of light. When the radiation enters the earth's atmosphere, as tenuous as it may be, the air may have a profound effect upon it. The earth's atmosphere affects not only the speed of the radiation, but also its intensity, spectral distribution, frequency and direction. All radiation, whether incoming or outgoing, is either scattered, absorbed, reflected, refracted or transmitted. The task of remote sensing is to understand the basic matter and energy relationships influencing these phenomena, to design detectors to record the process and to develop interpretation techniques for converting the data to usable information. A simplified model of the fate of incoming radiation on a stylized scene is given in figure 1-3.

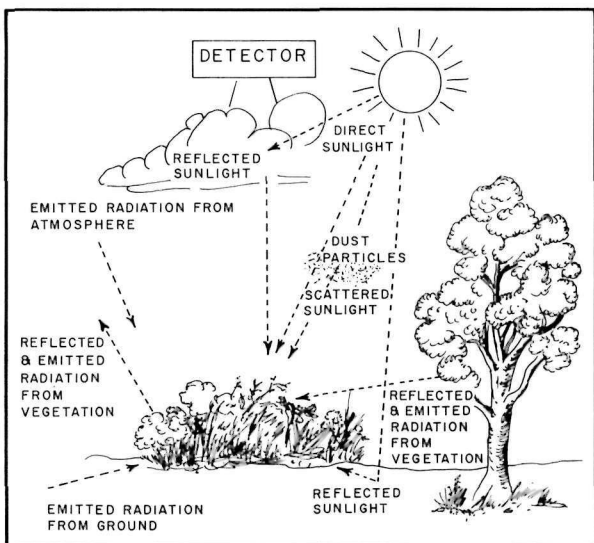
Scatter. There are four types of scatter: Rayleigh, Mie, non-selective and Raman.



1-2 The electromagnetic spectrum.

Table 1-1. Spectral regions, sensors and remote sensing platforms

| Region | Sensor | Platform |
|-------------------|------------------------------|------------------------------|
| Ultraviolet | Scanner/Camera/Radiometer | Aircraft/Handheld |
| Visible | Multispectral Scanner/Camera | Aircraft/Spacecraft/Handheld |
| Thermal Infrared | Scanner | Aircraft/Spacecraft |
| Passive Microwave | Radiometer | Aircraft/Spacecraft |
| Active Microwave | Radar | Aircraft/Spacecraft |



1-3 Model of incoming electromagnetic radiation.
Modified from NASA Facts NF-56/1-75.

Rayleigh scatter is caused mainly by air molecules and other minute particles that are smaller than the wavelength of the incoming radiation. This type of scatter is produced by the process of absorption of the radiation by a particle and the subsequent reemission of the radiation in a similar or totally different direction. There is no known method of predicting the direction of the reemission. Rayleigh scatter is inversely proportional to the fourth power of the wavelength. This means that ultraviolet light, which is almost one-fourth the wavelength of visible red light, is scattered sixteen times as much, and blue light four times as much (Nunnally, 1969). Rayleigh scatter is most evident on clear, cloudless days and is responsible for the blue color of our skies.

Mie scatter occurs when incoming radiation

comes into contact with relatively spherical particles with diameters approximately equivalent to the radiation wavelength. The main scattering agents in the visible light region are water vapor, dust particles and other particles ranging from several tenths of a micron to several microns in diameter. The total amount of scatter caused by Mie scatter is greater than Rayleigh scatter and involves longer wavelengths. It accounts for the blue haze over mountains, red sunsets and similar phenomena.

Non-selective scatter results when incoming radiation encounters atmospheric particles whose diameters are several times larger than the radiation wavelength. This scattering process is, therefore, non-selective with respect to wavelength. The water droplets in clouds scatter all visible light wavelengths equally, thereby giving clouds their white color. White is actually the presence of all colors . . . a point that will assume greater importance in section 3.

Raman scatter is the least important of the four types of scatter as far as remote sensing is concerned. It occurs when a photon has a partially elastic collision with a molecule, is deflected and loses energy.

Absorption. Many of the wavelengths of the electromagnetic spectrum, primarily the infrared and shorter-than-visible wavelengths, are affected much more strongly by absorption than by scatter. When energy of the same frequency as an atom or molecule is absorbed by a particle, it is converted and reemitted at a longer wavelength. The reemitted energy may be recorded in the form of luminescence, which occurs when electrons are boosted to higher energy levels, or in the form of heat. An excellent example of this is the well known "greenhouse effect" in which short wavelength radiation enters a structure, is absorbed, and later reemitted as heat at longer wavelengths.

Refraction. Refraction is defined as the bending of light as it passes from one medium into another. The amount of bending is dependent upon the angle at which the electromagnetic radiation strikes the boundary, the path length through the medium, and the densities of the two media involved.

At first glance, refraction may not seem important; but, when precise locations are being plotted, one needs to take its effects into account. Most plotting errors traceable to refraction occur when viewing from high altitudes or from shallow angles. The problem becomes even more severe in a turbulent atmosphere where the angle of refraction becomes unpredictable. Imagine the difficulties in plotting shallow underwater archeological features from aerial photographs.

Reflection. The term reflection refers to the process of "bouncing off an object." In remote sensing, the measurement of reflected radiation constitutes a large portion of research and study.

The ability of a surface to reflect depends on three primary factors: the angle of incidence, the refractive index, and the extinction coefficient. The amount of reflection, at least in the visible part of the spectrum, decreases as the angle of the incoming radiation approaches the vertical. For the radar region, just the opposite is true. These relationships are demonstrated by shining a light into a smooth water surface. If visible light is directed vertically into the water, very little is reflected; but, when illuminated at a more oblique angle, the reflection greatly increases. In the radar wavelengths, reflection (called backscatter) is greatest at vertical incidence and essentially zero at oblique angles.

The refractive index of a surface is its ability to bend incoming radiation. If a surface has a high refractive index, it means that a relatively high amount of incoming radiation is deflected through the surface and a low amount is reflected. Reflectivity at any given angle is directly proportional to the refractive index. When light strikes a transparent medium at vertical angles, the amount of reflection is almost entirely a function of the refractive index.

The extinction coefficient of a body refers to its ability to attenuate or dissipate radiation. This coefficient becomes important when evaluating the trade-off between spectral sensitivity and spatial resolution. When sensing from low altitudes, the layer of atmosphere is relatively thin and the extinction coefficient is correspondingly low. Under these conditions, spatial resolution is high. When viewing from orbital altitudes, the atmospheric layer is much thicker and, therefore, the extinction coefficient or

attenuation of the radiation is much higher. As a result of this, the spatial resolution greatly decreases and much more reliance must be put on spectral rather than spatial information when interpretation is undertaken on orbital imagery. As the spatial resolution decreases, larger and larger area units must be analyzed in order to make effective interpretations.

Electromagnetic Radiation Considerations in Archeology

Sensors. As archeologists evaluating the use of various sensors, we should have a firm idea as to exactly what our needs are. This publication is organized around the assumption that many archeologists will be researching prehistoric and ancient features that are not easily visible from the ground. Many will be looking for undiscovered structures and patterns rather than evaluating or measuring known structures. The latter case is complemented much more adequately by the art of aerial photogrammetry than by the more esoteric forms of remote sensing to be discussed here.

When we begin an investigation of a new area, we are usually looking for cultural features which manifest themselves on the surface as subtle differences in color or tone. These subtle differences may take the form of soil color variations due to extended tilling, crop marks, or possibly burn scars or cleared areas. We will also be looking for linear features such as old roads, footpaths, ditches and rectangularly shaped features such as structures. It will become more obvious in later sections of the supplement that certain sensors will complement our needs very well while others, whether due to high cost, poor resolution, or some other attribute, will be of little or no use. The exact nature of our specific interests and how the capabilities of each sensor can aid investigation should be kept in mind.

Processing. Once a sensor is chosen and imagery or other data are obtained, the question of processing techniques becomes paramount. Aside from basic image interpretation, there are numerous additional interpretation techniques, strategies, and devices which can be employed to draw from the image much more than is visible with the unaided eye. Many of these techniques will be explored in the following sections. It will be important to keep in mind the different ways in which an image can be manipulated and analyzed, since it may have a bearing on the type of imagery or data we will ultimately want to obtain.

Sensor Review and Applications in Archeology

Within the wavelength region from 200 nanometers (nm) (2×10^{-7} m) to approximately 1 meter, devices have been developed for recording reflected and emitted radiation from terrain objects. The sensors employed to record this energy in the form of images are classified either as cameras or as scanners.

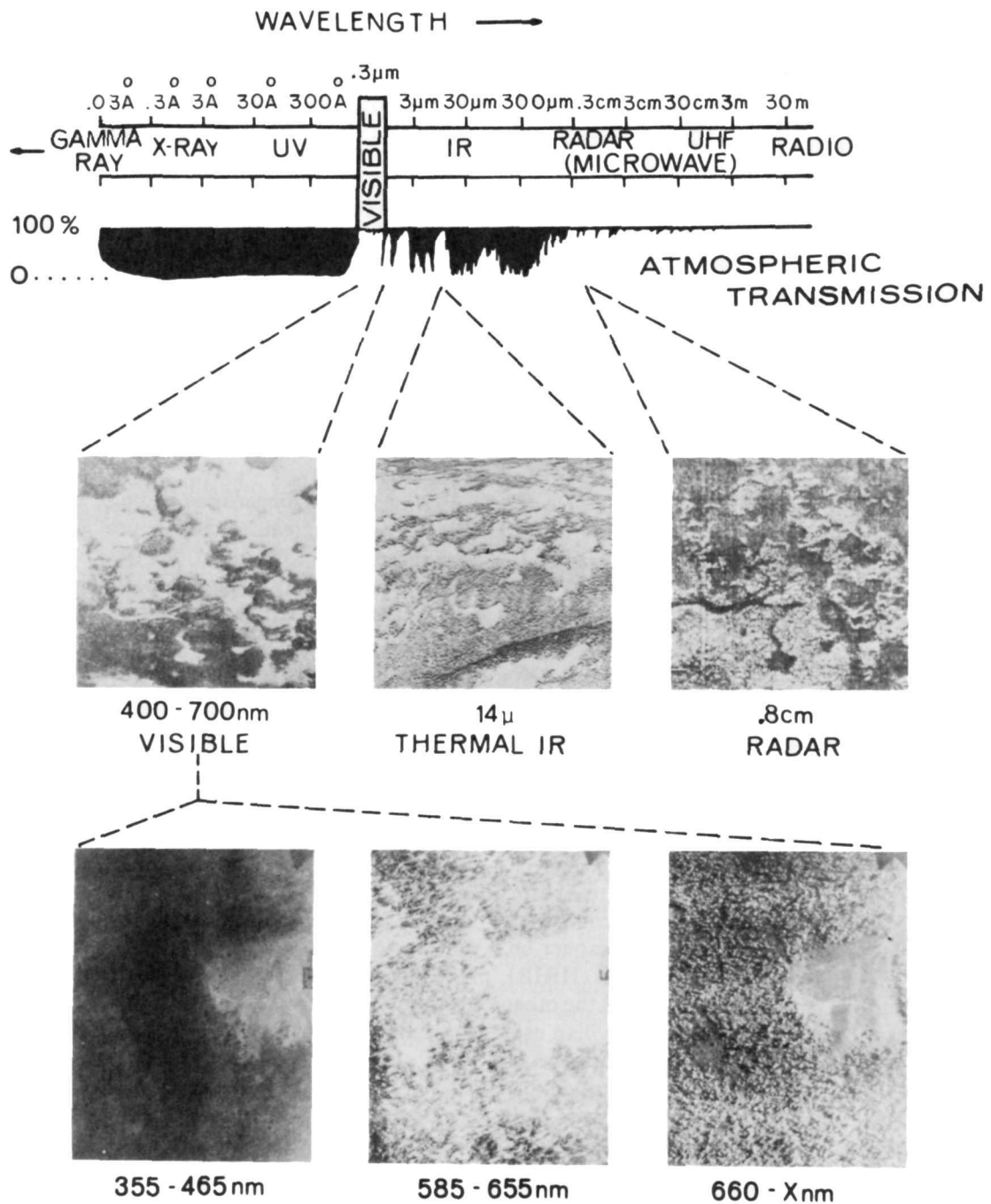
Non-imaging sensors such as magnetometers, scatterometers and radiometers provide point or line data, which, through manipulation, can be converted into map or image form. This section concentrates on sensor design and image interpretation of scanner imagery only, and will focus particularly on the ultraviolet, thermal infrared, passive microwave and radar regions of the spectrum. Multispectral scanners, particularly those on board Landsat I and II, will be discussed as a special design.

Reference is not made specifically to sensor platforms. Except for the multispectral scanner on-board Landsat I and II, the 13-channel scanner on Skylab, and the High Resolution Infrared (HRIR) sensors on-board weather satellites, none of the other scanners has yet been tried in space for civilian use. The reader should be aware of the importance of platforms (e.g. low, medium and high altitude aircraft; balloons; satellites; cherry pickers; etc.) because they directly influence not only image scale but also spatial and spectral color resolution. The higher the altitude, the more sensitive a detector must be to record reflectance and emission. Eventually, a trade-off point will be reached between the minimum size object we can image and the amount of reflected or emitted radiation given off by that object in a given part of the spectrum. Once that point is reached, we must sacrifice either spatial or spectral resolution. In the past, earth scientists have generally opted for greater spatial resolution and relied on object shape and scene context as prime interpretive aids. More recently, however, we have begun to

realize the importance of subtle tonal changes on the landscape and directed our attention toward greater spectral sensitivity.

Wavelengths longer than those in the reflective infrared region (greater than 900 nm) and those on the shorter side of the ultraviolet (less than 290 nm) cannot be imaged by direct photographic means due to the insensitivity of film emulsions to these regions. However, emitted and reflected energy in nearly all spectral regions can be *indirectly* photographed by scanning devices. Scanning devices provide many advantages over conventional photographs. In the infrared, passive microwave, and radar regions of the spectrum, imaging can be done at night as well as during the day. Another attribute is that scanner data are recorded electronically and, to some degree, noise and interference can be electronically subtracted. Figure 2-1 shows examples of imagery from the visible, thermal infrared and radar portions of the spectrum. Only the thermal IR and radar chips were produced by scanners; the others are photo images. The photograph at top left is a conventional panchromatic view of the terrain; the three lower photographs represent film/filter "slices" of the same general area. From left to right are depicted the ultraviolet, red and infrared views respectively. All of these images can also be obtained by scanning methods.

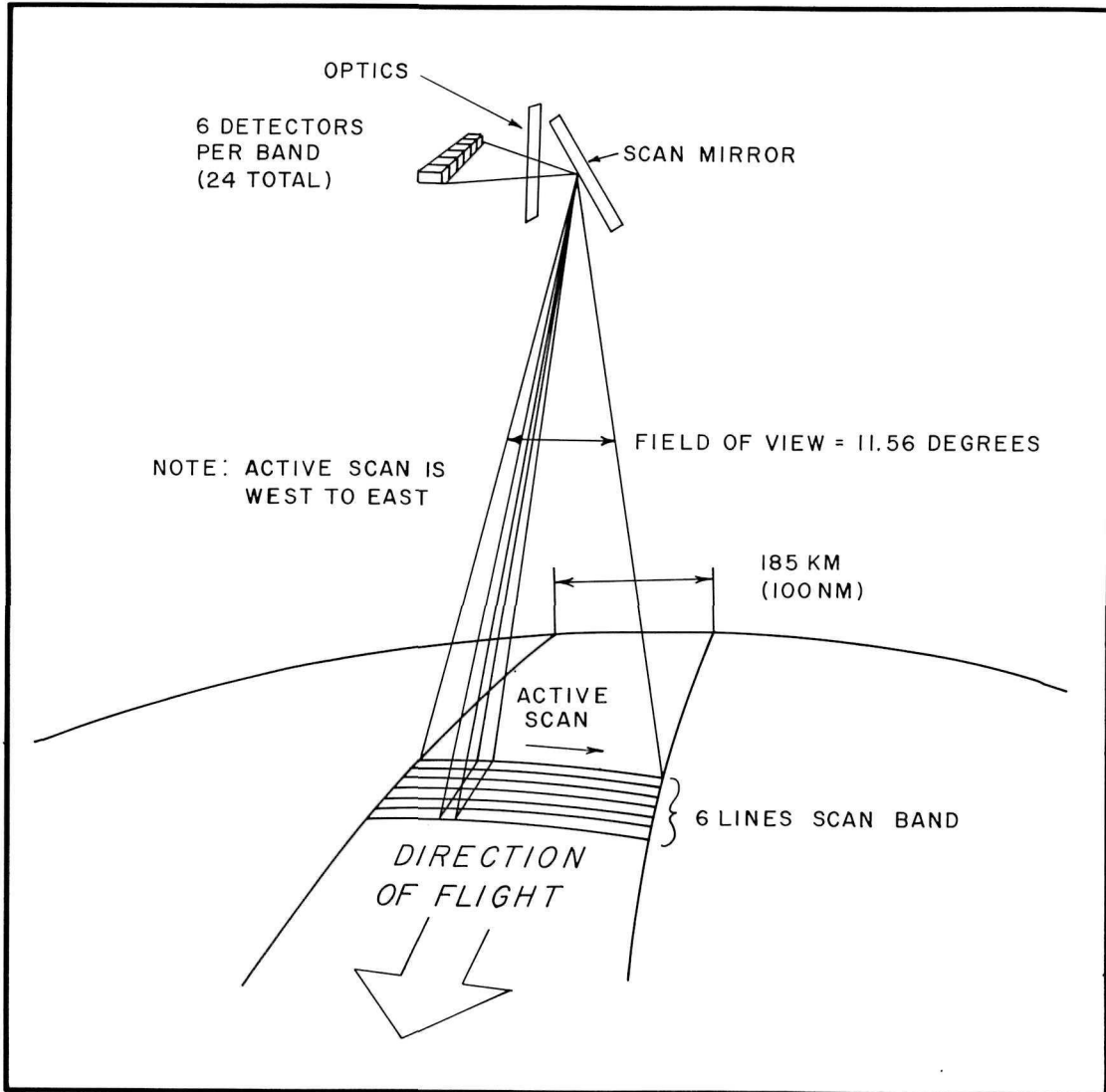
Line-scan systems (scanners) are optical mechanical devices that produce what is generally called "electronic imagery." These sensors are capable of operating in spectral regions from the ultraviolet (UV) through the far infrared, limited only by the ability of the earth's atmosphere to transmit energy signals in certain atmospheric "windows". Scanners are set up to collect data in one or more spectral bands (channels) depending on the number and type of detectors used. One research scanner system employed at NASA's Johnson Space



2-1 Examples of imagery from the visible, thermal, and radar portions of the spectrum. *Source: Morain, 1974.*

Center in an NC-130 aircraft has 24 channels. Other aircraft scanners are single or dual channel, normally in the thermal infrared portion of the spectrum, or are multi-channel systems with up to 10 or 12 bands.

A four channel multispectral scanner (MSS) is the primary sensor on board the Landsat satellites and a 13 channel system was flown on the Skylab missions.



2-2 Schematic of Landsat multispectral scanner (MSS). *Source: General Electric-Space Division.*

The principle of operation of most scanners is a rapidly rotating or oscillating mirror that scans across the line of flight collecting incident energy that is reflected or emitted from the ground surface (fig. 2-2). Through a set of optics, this energy is focused on one or more detectors that are sensitive to the desired wavelength bands. The variations in signal strength as sensed by the detectors are amplified by electronics and recorded. The recording can be done by one of two methods. An on board image record can be created by having the signals from the detector(s) modulate a cathode ray tube and by driving photographic film past these light forming devices proportional to the scan rate and forward motion of the platform. This creates a line-by-line display of the energy values. Another method, usually used for multi-channel systems, is to record the signals on magnetic tape and then process the data into an image format on the ground.

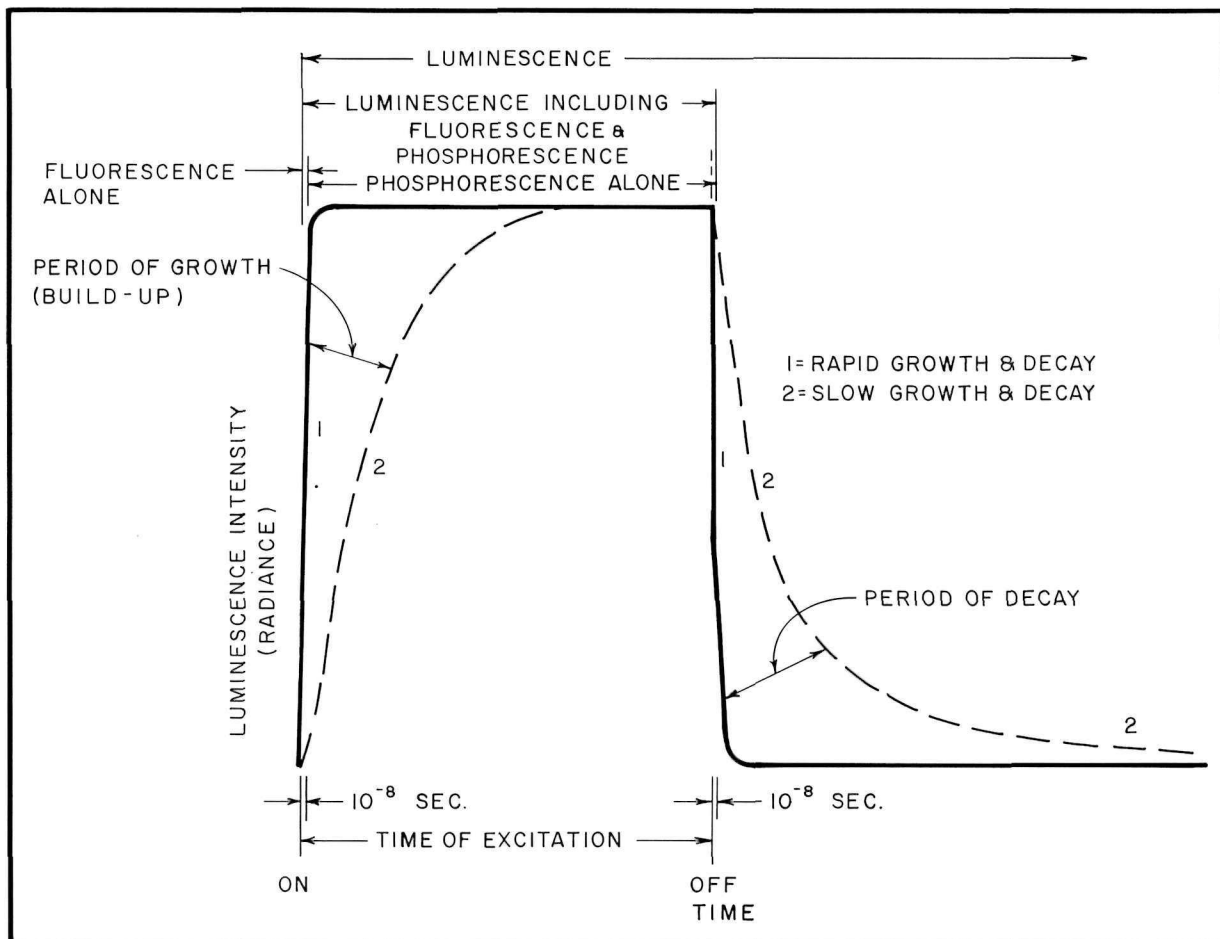
Ultraviolet

Sensor Operation. The ultraviolet region is defined as lying between the X-ray and deep purple end of the visible spectrum; that is, between 4 and 380 nm. In terms of the earth sciences, relatively little investigative effort has been expended on this part of the spectrum, either in the areas of sensor design or image interpretation. This situation arises primarily from two limiting factors of the atmosphere and one technical problem of sensor design. Ultraviolet radiation is greatly effected by Rayleigh scattering, or scattering caused by particles smaller than the radiation wavelength. It is also absorbed by gases such as ozone and molecular oxygen. In fact, these are the mechanisms that protect terrestrial life from harmful overexposure to ultraviolet radiation.

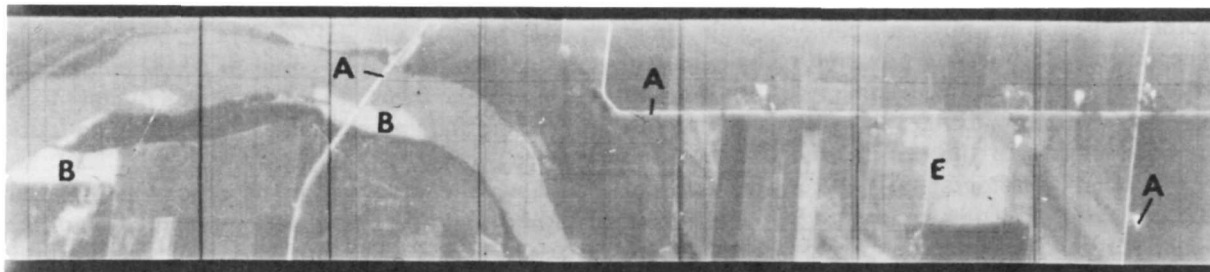
The critical technical problem in ultraviolet

sensing is that, at wavelengths shorter than 300 nm, ordinary glass cannot be used for camera lenses. They are opaque to ultraviolet and hence do not transmit the radiation. Special materials made from quartz or fluorite are transparent down to 120 nm, but at wavelengths shorter than this, it is difficult to find suitable material for lenses. Optical-mechanical scanners, of course, do not have a lens limitation because the radiation is recorded by a detector, not transmitted through a lens.

Basic Image Interpretation. The fundamental energy-matter relationship in the ultraviolet region is governed by electron shifts. Incident UV radiation, whether derived from the sun, from an air-borne pointable laser, or from an artificial light source, has the effect of displacing electrons to a higher and more unstable energy level. When these "excited" electrons return to their preferred status, they release this excess energy in the form of light. Luminescence is the observed result. Fluorescence



2-3 Diagram of luminescence emission and the relationships of growth and decay. Modified from *Manual of Remote Sensing*.



2-4 Sample of ultraviolet scanner imagery. (A) cultural features; (B) sand bars and bare fields; (E) area of tonal variations. Courtesy University of Kansas, Center for Research, Inc.

and phosphorescence are both forms of luminescence as illustrated in figure 2-3. Objects are said to fluoresce if their luminescent intensities increase and drop-off instantaneously with a burst of UV radiation (within 10^{-8} sec). Phosphorescence occurs in objects that have a slower response time and exhibit a lingering "glow" after excitation. We are all familiar, perhaps, with the beautiful "glowing" minerals displayed at gem and mineral meetings, county fairs and the like. These are examples of fluorescent and phosphorescent materials excited by an ultraviolet light.

In practice, it is not possible, using a UV scanner, to distinguish between these forms of luminescence because we are using the sun as our illuminating source and recording a continuous response. Many terrain features are luminescent over a broad range of wavelengths. Insufficient spectral data are available, however, to match observed grey tones on an image with specific features; consequently, only relative interpretations can be made for most landscapes.

Figure 2-4 is a sample of ultraviolet scanner imagery. The scene is of an agricultural area in the Midwest and shows a portion of the Kansas River to the left. Throughout the image, the greater the ultraviolet response, the brighter the resulting tone. Cultural features such as roads, houses, and bridges (marked as A) tend to have relatively high luminescence compared to agricultural fields. Likewise, sand bars and bare fields (marked as B) are more highly luminescent. Vegetated surfaces tend to be less luminescent; and standing water is moderate.

Applications in Archeology. For archeology, the features of prime concern in figure 2-4 would probably be subtle tonal variations of the type indicated at E. Areas of disturbed earth, old road nets, abandoned agricultural fields and similar features

might serve as clues to prehistoric or ancient occupation. As will be explained in section 3, these subtle tones and patterns can be enhanced by a number of techniques to facilitate their detection and interpretation.

The scattering of ultraviolet energy, usually a hindrance to the wider use of these sensors, can be used to an advantage in areas of rough terrain to "see" into areas of prolonged or deep shadow. It is also useful when only early morning (long shadow) photography is possible (Stringham and Williams, 1970). The pictures produced might not be visually pleasing because of overexposure in the sunlit portions, but the shadow areas would retain much of their information content.

In addition to shadow penetration, ultraviolet sensors can aid archeology in soil and site analysis. Cronin and others (1968) have found that quartz and calcite are more responsive in the ultraviolet than most other mineral types. Since limestone and marble were the common building materials of many past civilizations, it has been suggested that this higher response could help in locating new sites for excavation (Bevan, 1975).

Ultraviolet scanners could provide helpful information to archeologists. Even with the attendant problems of scattering and absorption, the ultraviolet spectrum does provide data, the content of which may contain information not obtainable in other portions of the spectrum. This added information, when combined with knowledge gained from other wavelengths, could help to identify objects or patterns on the ground.

Multispectral Scanners (Landsat)

Sensor Operation. For remote sensing in general, we are basically concerned with the question of how

much information we can obtain about phenomena without being in physical contact with those phenomena. All the interpretation techniques rely heavily upon the relative colors (spectra), sizes and shapes (spatial) and rates of change (temporal) between objects in the same scene. Conventional panchromatic photography is largely restricted to use of spatial relations with only secondary use of tone as a discriminant. The question of how much more we get from spectral and temporal analysis is now being explored, and one of the devices being used is the multispectral scanner.

Multispectral scanners have as their conceptual basis the premise that each terrain type in a given scene has an identifiable spectral signature or "fingerprint". We can discover what those fingerprints are by partitioning the optical and infrared portions of the spectrum into discrete bands so as to record the reflectance or emittance properties of each entity in each band, and select only those necessary for unambiguous identification.

Possibly the best known and most successful multispectral scanners are those aboard Landsat I and II. These scanners record energy reflected from the earth's surface in four spectral bands (or channels): the green (500-600 nm), the red (600-700 nm) and two bands in the reflective infrared (700-800 nm and 800-1100 nm). As the satellite passes over, radiant energy from the earth reflected in these wavelengths falls incident onto an oscillating mirror. This energy is recorded for each band by a bank of detectors, and after passing through an analog-to-digital converter, is either stored on magnetic tape or telemetered directly to a ground receiving station. The important design parameters for Landsat I and II are given in Table 2-1.

Each frame of imagery from Landsat shows an area on the ground of 185 km². From considerations of mirror scan time for each line of data, sampling time for each point in the line and the total time it takes to scan a complete image, one can calculate the nominal resolution of the system (Table 2-1). Landsat resolution cells are referred to as picture elements or "pixels" and are nominally given as 80 meters square or about 1.1 acre. For each pixel in each of the four channels, a reflectance value is recorded.

When the received energy is converted from raw voltage into digital format, it is "sampled" with 6 bit (2^6) accuracy; that is, the strength of the signal for each pixel in each band is converted to one of 64 binary numbers or grey levels. It is these binary numbers that are telemetered to earth for reconversion into data tapes or images. A radiance of zero

volts would have a digital count of 0; 2.5 volts would be midrange, or a digital count of 32; and saturation (5 volts) would have a count of 63. These radiant values are the focus of attention in all digital image processing and are especially valuable in band ratioing (see Section 3).

Several corrections should be made to Landsat imagery to obtain an accurate representation of the ground surface. These corrections are: rectification, haze correction, solar illumination and radiometric correction.

Rectification is a geometric correction for registering the image to a base map. Haze corrections are made to reduce atmospheric scattering, while solar illumination correction adjusts for average brightness across the entire frame. Lastly, radiometric corrections are necessary because six image scan lines are obtained in each scanning sweep of the mirror. Each of the six lines in each channel is recorded by a different detector. A problem arises because the six detectors for a given channel do not produce identical output for a given spectral input. The correction is accomplished by choosing one detector as a standard and adjusting the output of the other five detectors to meet that standard.

Basic Image Interpretation. The bandwidths on Landsat were selected for their specific information content. Reflected energy in the green channel¹ gives information on the density of vegetational cover, sediment loads in water and surface bare areas. The red channel is the chlorophyll absorption band and is useful in terrain analysis because healthy plants have low reflectance (synonymous with low voltage and low digital values). The reflective infrared channels (700 to 800 nm and 800 to 1100 nm) are useful because of the high voltages and digital counts observed for healthy vegetation and the much lower values observed for bare ground. Standing water absorbs the energy in this wavelength region and appears black (zero voltage and zero digital count).

To date, the overwhelming bulk of visual interpretation of black-and-white Landsat images has been in vegetation, soil, agriculture, hydrologic and geologic mapping. The techniques employed often focus on standard photo interpretation aids like tone, texture, size, shape and context. To make

¹The green channel is most often referred to as channel 4; the red channel as channel 5, and the infrared channels as 6 and 7. It is not uncommon, however, for the set to be referred to as channels 1 thru 4 respectively.

Table 2-1. Orbital and sensor parameters of Landsat I and II

| Orbital Parameters |
|--|
| Altitude — 920 km |
| Cycle of Duration — 18 Days (251 Revs) |
| Inclination — 99 Degrees |
| Sidelap Between Orbita — Equator - 14%, 30° - 25%, 60° - 57%, 80° - 85% |
| Endlap Along Track — 10% |
| Period of Orbit — 103 Minutes |
| Orbits Per Day — 14 |
| Area Covered Per Frame — 34,225 Sq. km |
| Time of Overpass — 0930 Local Sun Time Approx. |
| Sensor Parameters |
| Mirror Scan Time (one complete cycle) — 73.42×10^{-3} sec. |
| Active Scan Time ($\frac{1}{2}$ cycle) — 36.71×10^{-3} sec. |
| Sample Time — |
| $\frac{\text{number of samples per line}}{36.71 \times 10^{-3} \text{ sec.}} \times \frac{1 \text{ sample}}{9.95 \times 10^{-6} \text{ sec.}} = \frac{3,688 \text{ samples}}{\text{line}}$ |
| Pixel size (horizontal dimension) — 185 km / 3,240 samples per line (nominal) = ± 57 meters |
| Scene Scan Time — 25 sec. |
| Lines Per Scan — 6 |
| $25 \text{ sec./ band} \times 1 \text{ scan} / 73.42 \times 10^{-3} \text{ sec.} \times$ $6 \text{ lines/scan} = 2,040 \text{ lines/band}$ |
| Pixel Size (vertical dimension) = 185 km / 2,340 lines (nominal) = ± 79 meters |
| $3,240 \text{ pixels/ line} \times 2,340 \text{ lines/ band} = 7.6 \times 10^6 \text{ pixels/ band}$ |

more effective use of the spectral data as well as of the repetitive coverage every 18 days (or 9 days when one considers that Landsat I and II are 9 days out of phase with each other), a number of analog and digital image processing techniques have been developed to enhance subtle differences between images that might otherwise go unnoticed. These are discussed more fully in Section 3. As an entree into this array of techniques, we will, at this point, simply describe the interpretation of standard false color composites—so called because vigorous vegetation is displayed in shades of intense red rather than green.

Plate 1 illustrates the essential points of Landsat interpretation. The terrain features chosen include vegetation (coniferous and deciduous), water (clear and sediment-laden), bare soil and cloud. The “chips” indicate where on the scale of continuous tones one would expect to find each terrain item on each channel. When these are translated into combinations of yellow, cyan and magenta, exceedingly subtle colors result. Inspection of the diagram shows clearly that it is the tonal *difference* between

channels and the combination of those differences that we use for discrimination and identification. Those spectral differences need not be very great before they translate into clear distinctions as shown on Plate 2, an actual landscape in north central New Mexico.

Applications in Archeology. Applications of Landsat imagery in archeology are understandably limited. Archeological sites in North America are, for the most part, smaller than the nominal 1.1 acre pixel. Features such as ancient roads, trails, small agricultural plots and the like are also difficult to discriminate visually because of low scene contrasts. These remarks are based mostly on intuition, however, and not on the results of any systematic national survey. Certainly we should not close the book on this chapter before *non-visual* techniques are tried.

Lyons and Ebert (1976) of the National Park Service, Remote Sensing Division, have utilized Landsat imagery as a plotting base for the prehistoric road net converging on Chaco Canyon in

northwest New Mexico. The net was first observed on aerial photo enlargements and then transferred to satellite imagery. Some extension of the network was possible on the basis of interpretation and analysis of Landsat images. Edge enhancing, band ratioing and color enhancing are all methods for extracting additional information on such obscure features. All these techniques are discussed further in Section 3.

On a broader scale, the use of Landsat imagery could assist archeologists in a variety of ways. Regional surveys of vegetation, soils, surface drainage and topography are useful in the "convergence-of-evidence" approach to documenting possible sites. Such surveys are becoming routine not only because the Landsat data are available, but also because the locational information extractable from them meet USGS mapping standards at the scale of 1:250,000.

As a final note, Landsat I and II multispectral

scanners have only four channels and rather coarse resolution compared to airborne scanners. Other multispectral scanners having as many as 18 and 24 channels are available for use at aircraft altitudes and have resolutions comparable to standard aerial photographs. Table 2-2 gives a comparison of two such scanners, and figure 2-5 is a reproduction of the tonal renditions from 12 separate spectral regions. There is every reason to believe that image processing techniques can be used on data of this quality to discover new sites.

Thermal Infrared

Sensor Operation. There are three divisions of the infrared spectrum: the near, middle, and far (fig. 2-6). The near infrared (.7 μm -1.5 μm) is the reflected region and has been discussed in the *Handbook*; the

Table 2-2. Comparison of multispectral scanner bands and their significance for sensing vegetation (units are micrometers (μm) 1 μm = 10^3nm)

| System | Spectral Regions | # Channels Per Region | Vegetational Importance |
|--|--------------------------|-----------------------|--|
| Bendix 24 Channel Scanner;* scan $\geq 80^\circ$ | .34 – .5 μm | 3 | Inconclusive |
| | .53 – 1.05 μm | 7 | Green reflectance; chlorophyll absorption |
| | 1.18 μm | 1 | Plant vigor / stress |
| | 1.73 μm | 1 | Plant vigor / stress |
| | 2.1 – 4.75 μm | 3 | Forest fire mapping |
| | 6.0 – 13 μm | 7 | Inconclusive |
| | calibration | 2 | Inconclusive |
| University of Michigan 18 Channel scanner** | .32 – .5 μm | 5 | Inconclusive |
| | .5 – 1.0 μm | 8 | Green reflectance; chlorophyll absorption; plant vigor / stress |
| | 1.5 – 1.8 μm | 1 | Inconclusive |
| | 2.0 – 5.5 μm | 3 | Forest fire mapping |
| | 8.0 – 13.5 μm | 1 | Inconclusive |
| | | | |
| NASA Landsat scan $\leq 11^\circ$ | .5 – .6 μm | 1 | Center of green reflectance |
| | .6 – .7 μm | 1 | Center of chlorophyll absorption |
| | .7 – .8 μm | 1 | Plant vigor / stress |
| | .8 – 1.1 μm | 1 | IR reflectance |

* From: Stein, K. J., 1971, "Multispectral Scanner Promising," *Aviation Week and Space Technology*, May 24, pp. 39-41. (See also Zaitzeff, E.M., C.L. Wison, and D.H. Ebert, 1970, "MSDS: An Experimental 24-Channel Multispectral Scanner System," *Bendix Technical Journal*, 3(2):20-32).

** From: Holter, M.R., 1971, "Infrared and Multispectral Remote Sensing," Proceedings NATO AGARD Conference on *Propagation Limitations in Remote Sensing*, 17th Symposium held in Colorado Springs, June 21-25.

middle ($1.5\text{--}5.5\mu\text{m}$) is measured as a combination of reflected and emitted radiation; and the far infrared ($5.5\text{--}14\mu\text{m}$) is emitted radiation only. Thermal scanners are usually designed to measure narrow bands of emitted radiation in the $3\text{--}5\mu\text{m}$ or $8\text{--}14\mu\text{m}$ "windows".

All objects with a temperature above 0°K emit electromagnetic radiation. The wavelength of the maximum observed radiation is a function of the object's temperature. Heat generated by an object is, in fact, the result of the movement of molecules. The faster the molecules are accelerated, the more heat will be generated. Objects generally emit some amounts of all wavelengths but Wien's Displacement law (fig. 2-7) demonstrates that peak radiation moves to the shorter wavelengths as the temperature increases.

According to Wien's law, objects whose ambient temperature is in the range of 300°K (most earth features) should have a peak emission in the 8-

$14\mu\text{m}$ region. Sensing in this window provides an opportunity to detect subtle temperature differences on the order of 1 or 2°C . In contrast, scanners designed to operate in the $3\text{--}5\mu\text{m}$ window are sensitive to temperatures like forest fires (600°K).

Although referred to as thermal scanners, the detectors are actually recording emitted radiation, which is in turn related to the fourth power of the object's temperature:

$$\omega = \epsilon \sigma T^4 \quad \text{where:}$$

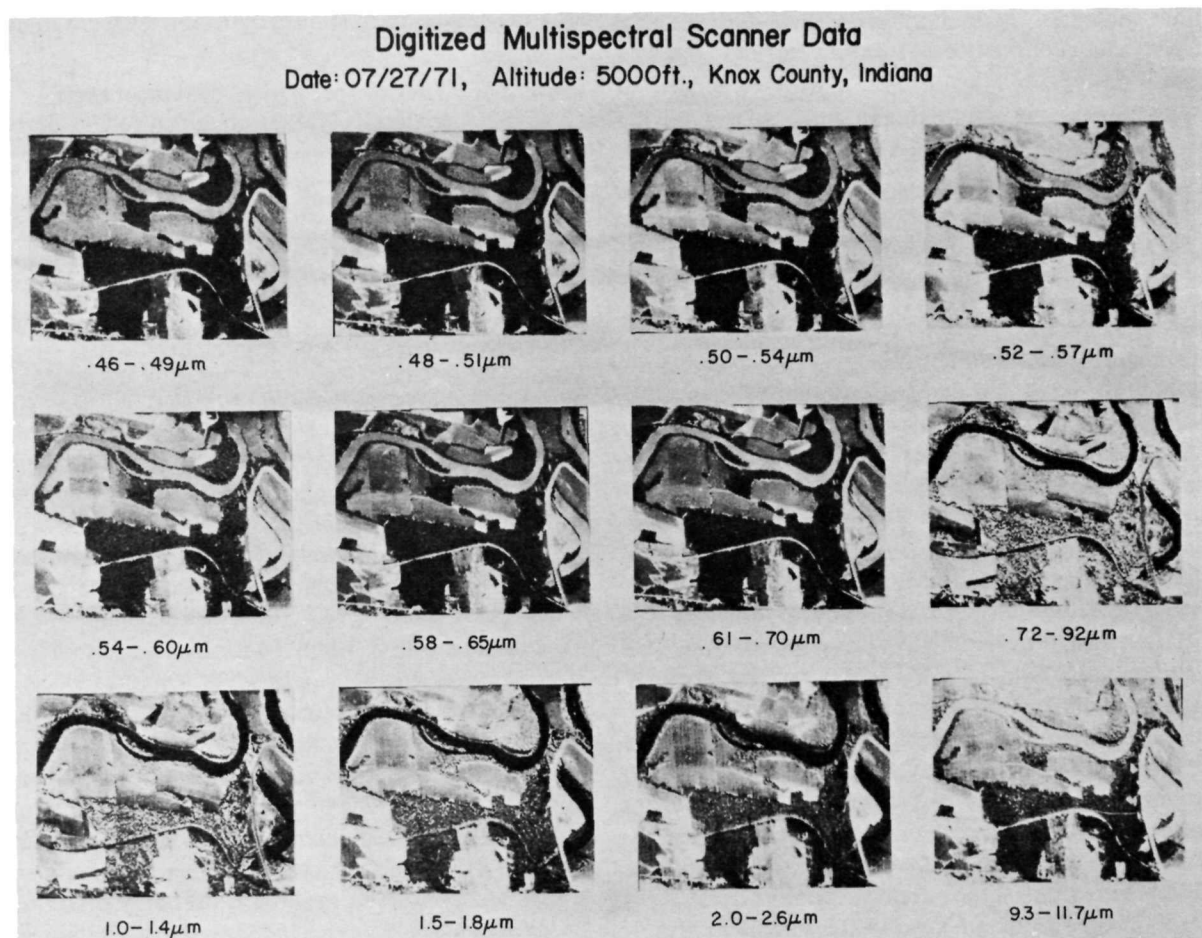
ω = Radiant flux emitted per unit area

ϵ = The emissivity of the object

σ = The Stephan-Boltzmann constant

T = Temperature ($^\circ\text{K}$)

From the above equation we learn that an object's emissivity is all important in thermal sensing; the more so in nearly isothermic landscapes. Emissivity is, in turn, a complex resultant of an object's thermal



2-5 Reproduction of tonal renditions of twelve spectral regions from a multispectral scanner. Courtesy LARS (Laboratory for Applications of Remote Sensing).

conductivity, thermal diffusivity, specific heat and thermal inertia. Table 2-3 gives the thermal properties of some typical rock materials.

We have seen in figure 2-6 that much of the infrared spectrum is opaque. This is due to water and CO₂ absorption. Even inside the windows, the atmosphere is not uniformly transparent. Rather, it acts as a selective attenuator of emitted energy. Moreover, the atmosphere itself is a strong radiator in certain bands and contributes to part of the signal received by the sensor. In order to function at all, the sensors must be designed to take this atmospheric "noise" into account.

All thermal scanners operate by using highly sensitive detectors that are cooled to nearly absolute zero (-273°C). The detector usually consists of a coating of mercury, copper, or gold-doped germanium or alloys like mercury-cadmium-telluride. For practical considerations, the image user is only interested in the value defined as the "noise equivalent temperature difference" (NEΔT). This value indicates the maximum sensitivity, or, in a sense, the radiometric resolution of the detector above the "noise" level. For a 300°K scene, an NEΔT of 1.5°K would mean that objects having temperature differences less than 1.5°K could not be distinguished unambiguously. The "dynamic range" of the scanner is another important parameter and is defined as the temperature gradient over which the detector is most sensitive, as for example, 260°K to 340°K.

Basic Image Interpretation. Imagery may be produced directly from the detected energy by using the strength of the signal to modulate the intensity of a light source in a cathode ray tube. As the aircraft moves forward along its path, energy incident upon the mirror is converted to an electrical impulse and displayed, line-by-line, on a television-like screen (fig. 2-8). Film is passed over the tube at a rate that is proportional to the speed of the aircraft and inversely proportional to its height above the ground. The instantaneous field of view (IFOV) is the nominal spatial resolution of the system. If one could stop the mirror at any given instant, the IFOV would be the area on the ground that would be contributing the detected energy. As the diagram shows, it is measured as a solid angle in square milliradians. A one square milliradian resolution for example is equivalent to one square foot at an altitude of 1000 feet, 6 inches² at 500 feet, or 600 feet² at 100 miles.

In general, thermal scan imagery (or thermography) can be interpreted qualitatively in terms of

tone (fig. 2-9A and B); i.e., lighter tones are warmer while darker tones are cooler. For natural landscapes, water and vegetated surfaces are cooler on daytime images than either bare soil or cultural features. One should be aware in discussing thermograms that temperature differences between objects are relative. Rock and mineral substances generally have wider diurnal temperature fluxes than do healthy biological phenomena. Plants and animals have evolved mechanisms to reduce the amplitudes of diurnal change to maintain a relatively uniform internal environment. Wider than normal temperature fluxes or persistently high or cold temperatures are therefore a good indicator of stress, either of moisture or disease.

For best image interpretation, one must consider and compare the thermal properties of relevant landscape elements. For example, the specific heat of water approaches 1; but for sandy soil, the value is 0.24, and for granite it is only 0.16. Consequently, solid ground will warm up faster after sunrise and cool off faster after sunset than will water bodies.

Table 2-3. Thermal properties of typical rock materials (values are given in Cgs units)

| | K | ρ | C | α | β |
|-----------------------|--------|-----|------|-------|-------|
| Granite | 0.0065 | 2.6 | 0.16 | 0.016 | 0.051 |
| Basalt | 0.0050 | 2.8 | 0.20 | 0.009 | 0.052 |
| Sandstone, qtz | 0.0062 | 2.5 | 0.19 | 0.013 | 0.064 |
| Limestone | 0.0048 | 2.5 | 0.17 | 0.011 | 0.046 |
| Marble | 0.0055 | 2.7 | 0.21 | 0.010 | 0.055 |
| Shale | 0.0030 | 2.3 | 0.17 | 0.008 | 0.034 |
| Sandy soil | 0.0014 | 1.8 | 0.24 | 0.003 | 0.003 |
| Clay soil (moist) | 0.0030 | 1.7 | 0.35 | 0.005 | 0.004 |
| Gravel | 0.0030 | 2.0 | 0.18 | 0.008 | 0.033 |
| Sandy gravel | 0.0060 | 2.1 | 0.20 | 0.014 | 0.050 |
| Dolomite | 0.012 | 2.6 | 0.18 | 0.026 | 0.075 |
| Gabbro | 0.0060 | 3.0 | 0.17 | 0.012 | 0.055 |
| Peridotite | 0.011 | 3.2 | 0.20 | 0.017 | 0.085 |
| Rhyolite | | 2.5 | | | |
| Pumice, loose, dry | 0.0006 | 1.0 | | | |
| Obsidian | | 2.4 | | | |
| Tuff, welded | 0.0028 | 1.8 | | | |
| Slate | 0.0050 | 2.8 | 0.17 | 0.011 | 0.048 |
| Quartzite | 0.012 | 2.7 | 0.17 | 0.026 | 0.075 |

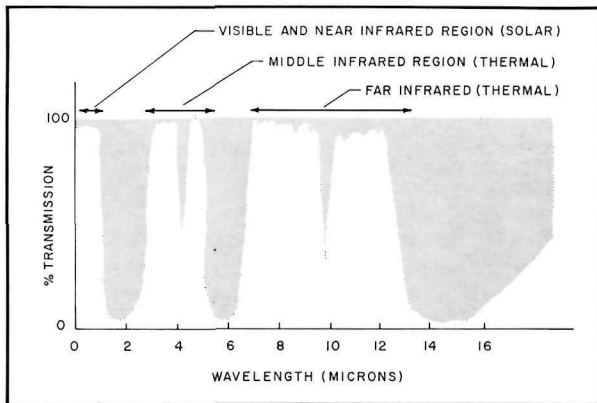
K = Thermal conductivity; measured as Cal cm⁻¹ sec⁻¹ °C⁻¹

ρ = Density

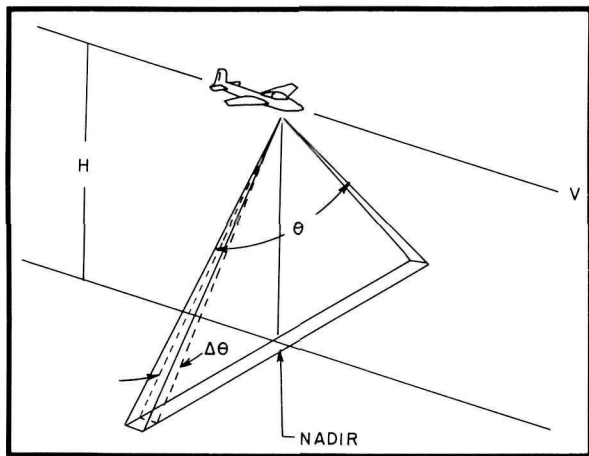
C = Specific heat; measured as Cal gm⁻¹ °C⁻¹

α = Thermal diffusivity; measured as cm² sec⁻¹

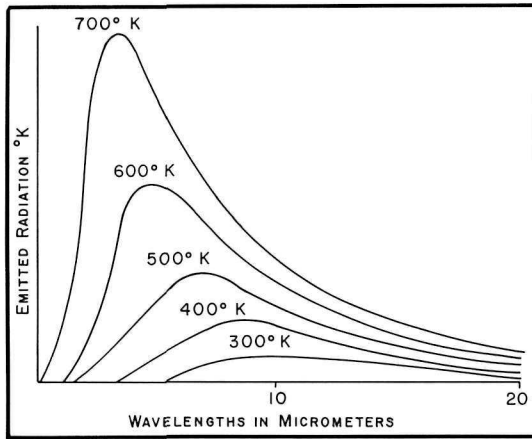
β = Thermal inertia; measured as Cal cm⁻¹ °C⁻¹ sec^{-1/2}



2-6



2-8



2-7

Daytime thermal images will, therefore, show water as relatively cool (fig. 2-9B), whereas nighttime images (fig. 2-9C) will show it as relatively warm (lighter toned). Conversely, daytime images show land as relatively warm and nighttime images will show it as relatively cool (darker toned). Although the tone renditions of water are "black" and "white," the actual temperature flux between day and night is quite small.

Notice on figure 2-9B and C that the paved road is easily visible at night as a relatively warm surface, compared to the cooler landscape, and that it continues to appear as a warm surface on the daytime image but is almost impossible to trace through the equally warm countryside. Paved roads appear in this fashion because the paving material has a low specific heat (meaning it warms up quickly) and an ability to reradiate that energy slowly throughout the night.

Much of the applications research in thermal infrared scanning has come from the mid and high

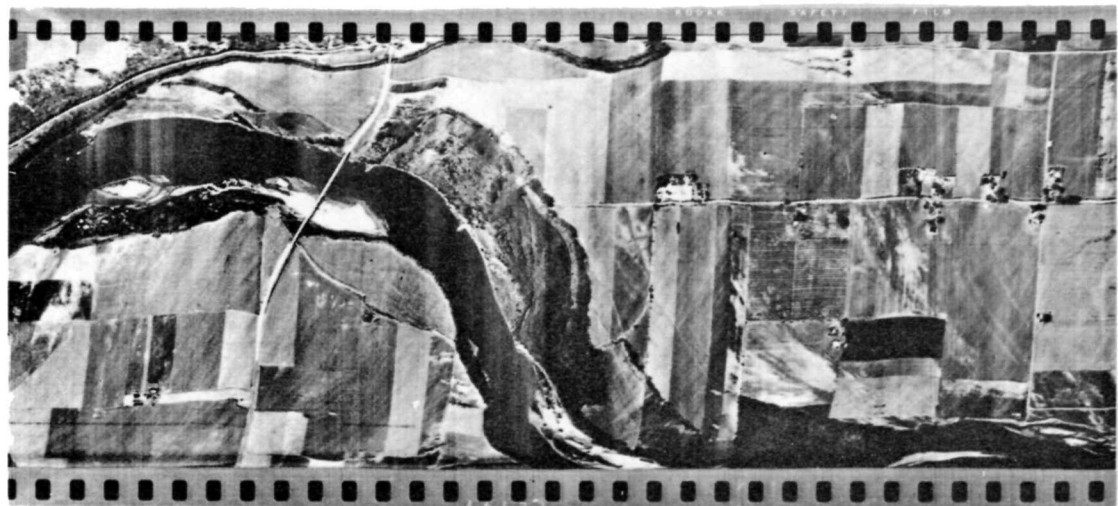
2-6 Divisions of the infrared spectrum. *Source: Morain, 1974.*

2-7 Wien's Displacement Law. *Source: Nunnally, 1969.*

2-8 Configuration for a typical infrared scanner. A scan mirror is rotated from side to side having a field of view of Θ and resolution of $\Delta\Theta$. The detector is cooled below zero and is thus sensitive to very minor changes in terrestrial emissivities. Relative emissivities of the scene below the aircraft are converted first to electrical signals, then to an intensity modulated light source, and recorded on film. The higher the emissivity (warmer temperatures), the brighter will be the light source and hence the tonal rendition on positive imagery. *Modified from Morain, 1974.*

latitudes, particularly over frozen terrain. Although temperatures of polar regions are much lower than elsewhere, the temperature differences between landscape elements are often much greater. Much work is being done in the $8-14 \mu\text{m}$ window to plot ice-water-land boundaries, delineate different types of sea ice, and differentiate currents and streams of varying temperature. In the $3-5 \mu\text{m}$ window, thermal infrared scanners can also be used to delineate geothermal areas, active volcanic regions and the burning fronts of forest fires.

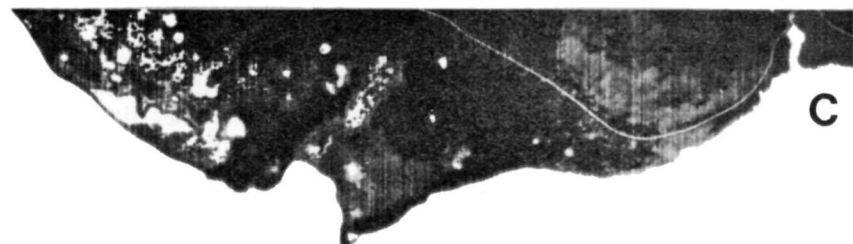
Applications in Archeology. Thermal infrared imagery has often been applied in archeology to detect ancient agricultural patterns. These are sometimes visible on imagery because patterns and vegetation regrowth have been altered by previous tilling methods. Growth marks are generally visible only during those times of the year when crops are growing in the fields or after a heavy rainfall when differences in soil moisture retention are highly con-



A



B



C

2-9 Examples of thermal infrared imagery:

- A. Daytime thermal image of same area shown in Figure 2-4.
- B. Daytime thermal image.
- C. Nighttime thermal image of same area as B. *Courtesy NASA.*

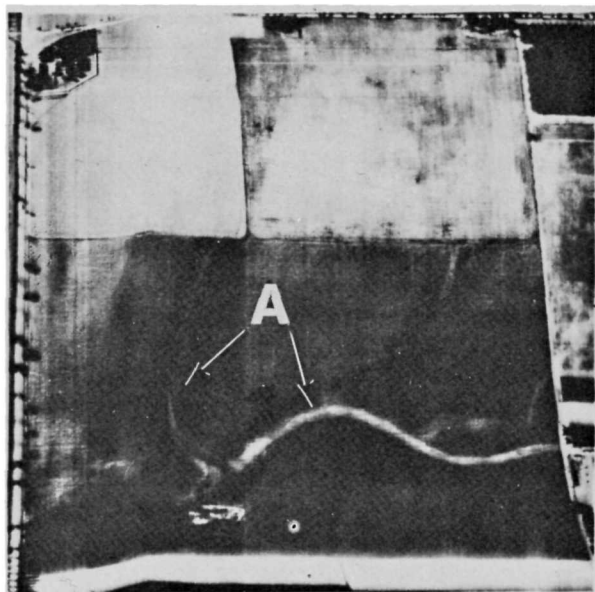
trasted. Patterns become visible in part because wet soils have a higher specific heat than dry soils and in part because former tillage practices may have sufficiently compacted the soil materials to alter their thermal diffusivities. Figure 2-10 illustrates the ability of thermal imagery to highlight soil moisture contrasts.

Schaber and Gumeran (1969) observed parallel linear light and dark features on thermal infrared imagery which were almost invisible on conventional aerial photos. Ground reconnaissance revealed the linear features to be old field plots with alternating rows of volcanic ash and soils. The ash rows had a lower thermal inertia, or rate of heat loss, and had a different appearance on the imagery than did the soils. Other features, such as buried ditches, sometimes appear to be warmer than their surroundings after sunset due to their higher heat content (Sabatini and others, 1971). This principle has also helped to locate springs in the desert (Wermund, 1971) and near surface groundwater (Chase, 1969).

Active Microwave Sensors

Sensor Operation. The microwave portion of the spectrum spans the millimeter and centimeter wavelengths. The shorter of these wavelengths are usually explored using passive microwave systems (discussed later in this section) while the longer ones, from about 1 cm. to 1 m., have been the focus of active systems called radar. Almost all of the current civilian radar systems use wavelengths from .86 cm (referred to as Ka-band) to 30 cm (referred to as L-band). This encompasses the range shown in Table 2-4.

The longer wavelengths of radar are attractive in remote sensing research because they not only enable data collection through overcast skies and during either day or night hours, but also because terrain itself can be penetrated to varying depths. This penetration capability is dependent on many factors among which the most important appear to be wavelength and surface moisture. Longer wavelengths of P and L band systems can penetrate dry sands to a depth of several meters. Shorter wavelengths (e.g. X and K-band) are mostly sensitive to surface, rather than subsurface, reflections. As the moisture content of the scene increases, depth penetration decreases sharply so that reflections from moist features are almost totally surface phenomena. The data in Table 2-5 shows calculated



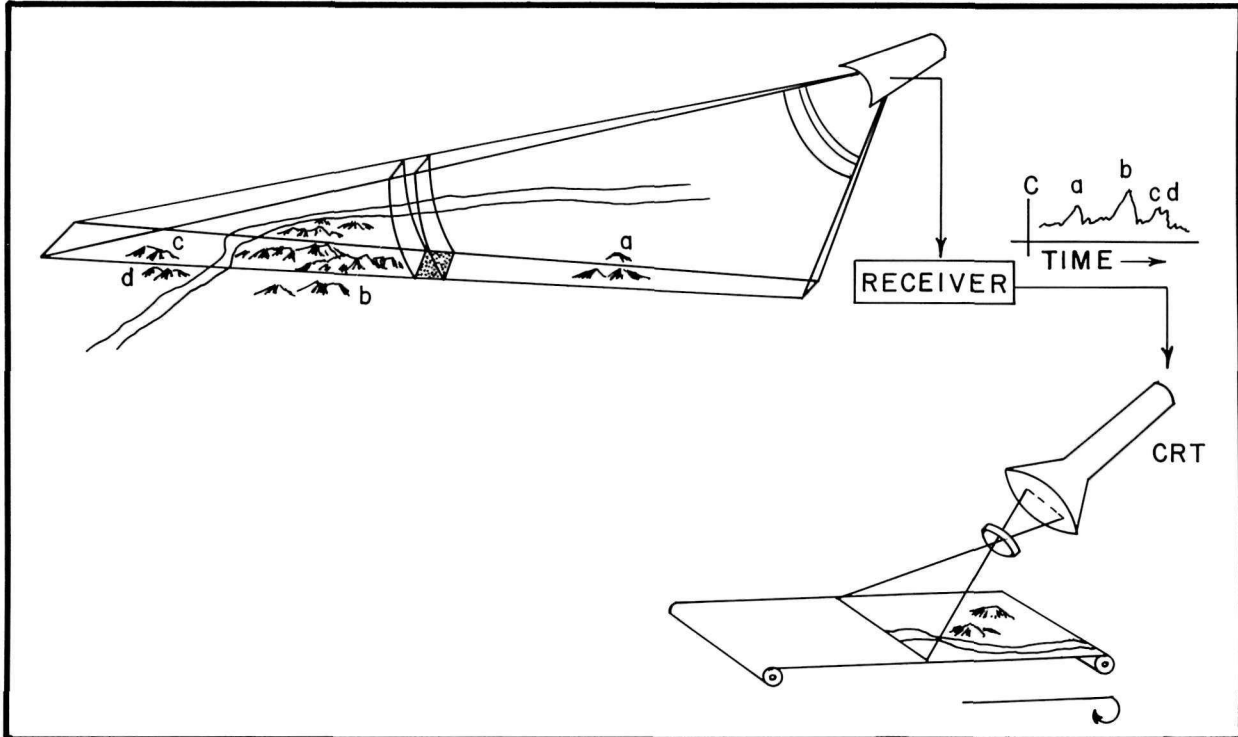
2-10 Thermal infrared imagery is very effective in detecting soil moisture variations. The letter "A" points to a buried river channel.
Courtesy Texas Instruments.

Table 2-4. Radar bands, bandwidths, and frequency ranges

| Band Designation | Bandwidth (λ in cm) | Approx. Corresponding Frequency Range |
|------------------|---------------------|---------------------------------------|
| Ka | .83-1.18 | 40-26.5 Gigahertz |
| K | 1.18-1.67 | 26.5-18 Gigahertz |
| Ku | 1.67-2.75 | 18-12.5 Gigahertz |
| X | 2.75-5.77 | 10.9-5.2 Gigahertz |
| S | 5.77-19 | 5.2-1.5 Gigahertz |
| L | 19.3-76.9 | 1.5-4 Gigahertz |
| P | 76.9-140 | .4-.2 Gigahertz |

depths of penetration for 3 soil materials at various moisture contents.

Radar sensors of the type commonly employed for weather monitoring and navigation (usually referred to as plan position indicators—PPI-radars) are true scanning systems in the sense that the antenna is rotated or oscillated to scan the area of interest. In remote sensing of terrain features, however, the side looking airborne radar (SLAR) is most often used (fig. 2-11). It can be considered as a scanning system but really is not. For SLAR sensors, the antenna maintains a fixed position. The "scan" to



2-11 Schematic of the SLAR system. In the upper left of the diagram, the surface features at a, b, c, and d reflect the radar impulse back to the antenna where they are recorded as electrical currents. The diagram of the electrical current intensities at the upper right shows that the reflectance intensities can vary considerably depending on factors such as slope and soil moisture. The electrical currents are then converted into a beam of light in a cathode ray tube as is shown in the lower right portion of the diagram. The beam of light is scanned over a strip of film and a radar image of the terrain surface is created. The brightness of the beam of light varies directly with the intensity of the electrical current.

the side of the aircraft is obtained by measurement of the time delay to and from the target; the "scan" along the flight line is obtained by synchronizing flight speed with film speed as in thermal scanners. Side-looking radar systems operate by transmitting a known signal and receiving that portion reflected back toward the receiver from objects on the ground. The basic radar equation (1) states that the power returned (P_r) to the receiver from any reflecting element is a function of the transmitted power (P_o), the gain of the antenna (G), the wavelength of the transmitted energy (λ), the reflection coefficient (σ) for that element, some function of the "look" angle and beam width (θ, ϕ), and the distance (R) to the target.

$$P_r = \frac{\sigma G^2 P_o \lambda^2 |f(\theta, \phi)|^4}{(4\pi)^3 R^4} \quad (1)$$

Each of the sensor parameters can be controlled so that the only variable is σ , the reflection coefficient of the specific ground object. In order to present this value as an area rather than a point value, it must be transformed. This is accomplished by averaging the return signal over an area and defining

Table 2-5. Depth of signal penetration in soils (meters)

| Type of Soil | Percentage of H ₂ O | P-Band $n = 1\text{m}$ | S-Band $n = 0.1\text{m}$ | X-Band $n = 0.3\text{m}$ |
|--------------|--------------------------------|---------------------------|-----------------------------|-----------------------------|
| Sand | 0 | 20 | 3.3 | 1.6 |
| | 3.88 | 5 | 0.33 | 0.046 |
| | 16.8 | 2.4 | 0.063 | 0.01 |
| Loam | 0 | 31 | 18 | 4.8 |
| | 2.2 | 2.8 | 0.43 | 0.19 |
| | 13.77 | 0.44 | 0.059 | 0.016 |
| Clay | 0 | 10.3 | 1.4 | 0.55 |
| | 20 | 0.14 | 0.038 | |

the value obtained as the backscattering cross-section (σ^o) (Equation 2, from Moore, 1970).

$$\sigma^o = \frac{(4\pi)^3 P_r}{P_o \lambda^2 \int G^2 dA |R|^4} \quad (2)$$

Black-and-white line scan imagery is produced by converting this basic quantity, σ^o , into a spot of light, which is regulated in intensity according to the strength of the received signal. A strong reflection will produce relatively bright tones, whereas a weak

signal will result in relatively dark tones. These tones are described as "relative" because at present they cannot be converted into absolute values. Nevertheless, relative values are useful if they can be interpreted vis-a-vis the factors determining reflection strength. These determining factors can be divided into (1) ground variables, and (2) system variables. The most important ground variables are the dielectric properties of the surface elements, largely determined by moisture content, and surface geometry, determined mostly by the surface composition, microrelief and vegetative cover. In addition, image interpretation must also take into account the microwave variables of wavelength, viewing angle, and resolution. Interactions between ground and system variables produce the tone and texture observed on the image. Because these interactions operate in a predictable fashion, they can be used as clues in image interpretation.

Basic Image Interpretation. Most radar imagery is evaluated by using standard photo interpretation techniques. The literature is generally not responsive to interpretation of images based on the microwave properties of the terrain and this arises out of a need for much more basic research. Enough is known or suspected about the interaction of certain terrain/sensor variables to make the following discussion possible.

For the interpretation of image tone and texture, there are basically three scales of reference to keep in mind. For simplicity, we will describe them here as "micro", "meso" and "macro" roughness.

The finest scale of reference, **microscale roughness**, is most important in the interpretation of image grey tone. Image tone is primarily a function of system wavelength, signal polarization, and viewing angle. Just as there are different amounts of blue, green and red reflectance between objects in the visible spectrum, so also are there differences in the radar spectrum depending upon which band is employed. Similarly, just as different objects have variable reflectances depending upon solar elevation, azimuth, and viewing angle, so too do they have different radar reflections as a function of angle of illumination. In addition to these sensor properties, there are microscale terrain properties such as leaf size, pebble size and distribution, branching patterns and object moisture content that also influence tone.

Mesoscale roughness is referred to by some as the "gross roughness envelope" and is directly related to image texture. Consider that if one had a

sufficiently large cloth and could drop it over a given surface, much of the high frequency (microscale) terrain roughness could be smoothed. Intuitively, if such a cloth were dropped over a forest, there would be large peaks and nulls resulting from the height variability between tree crowns and the open ground or understory cover. This same cloth, if dropped over a shrub or grassland type would have considerably less amplitude in the peaks and nulls.

The **system** variables that most influence texture are wavelength and resolution. Wavelength is important because the longer the wavelength, the greater must be the amplitudes comprising the envelope. System resolution is important because in envelopes of high roughness, the finer the resolution, the more prominent will be the resulting texture. Since resolution is achieved by averaging signal strengths over an interval of time, the finer the resolution, the greater the variability in average signals over a rough envelope, resulting in a finer texture.

The terrain parameters that influence image texture are associated with object sizes, shapes and arrangements. An open tree savanna with less than, say, 5 percent tree cover would probably image as though it were a grassland. An even-aged forest plantation should have an envelope of moderate amplitude and hence display less texture than an overmature forest having a mixture of old and young trees and variable spacings. Scenes having a mixture of height classes visible to the signal will probably have a compound texture.

Macroscale roughness refers to image patterns arising out of a combination of micro and mesoscale roughness superimposed on sloping terrain. Radar images are superior to any other form of remotely sensed data for depicting terrain configurations. Incredible details of drainage and other geomorphic features are highlighted by the fact that the system is side-looking and hence sensitive to surface undulations. While this fact is a boon to geomorphologists, it serves as a complicating factor for tone and texture interpretation.

Figure 2-12 illustrates the concepts of tone and texture on a K-band image. There are three types of vegetation shown on the image. These three have obvious differences in tone and texture that can be related back to micro and mesoscale attributes. The area marked A is a white fir (*Abies*) forest; that labeled B is a ponderosa pine (*Pinus*) forest; C indicates chaparral (*Arctostaphylos*) shrub; and D represents an area of ambiguity arising from slope influences. The mottled white and black area to the

left of the scene is a bog environment of grass and sedge.

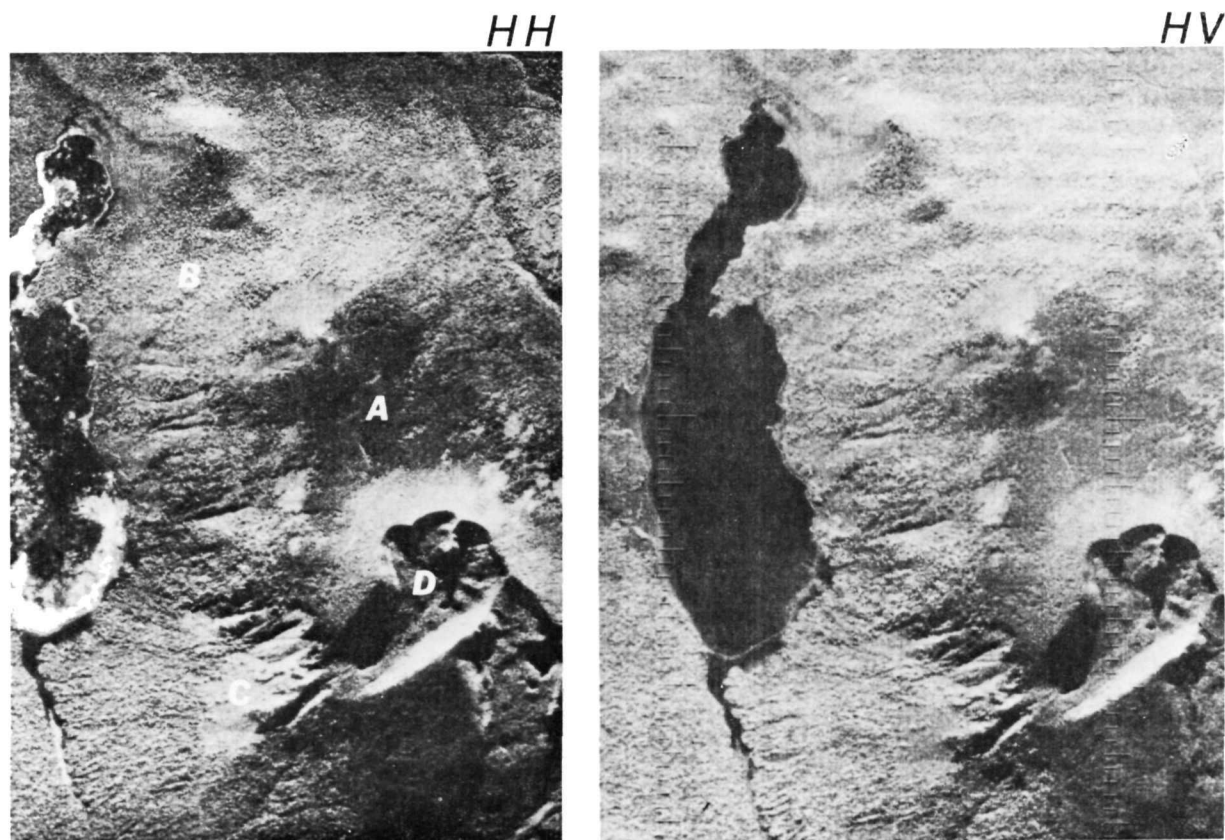
Signal polarization also has a strong influence on image tone and texture. For active microwave there are four possible polarizations: horizontal transmit, horizontal receive (HH); horizontal transmit, vertical receive (HV); vertical transmit and receive (VV); and vertical transmit, horizontal receive (VH). The HH and VV formats are referred to as the "like-polarized" images while the HV and VH are called "cross-polarized" images. "Horizontal" in this context refers to cases when the electric field of a signal is parallel to the surface; vertical means that the magnetic field is parallel to the surface (refer to fig. 1-1).

It can be shown that, given two polarized images (HH and HV), the HH will be dominated by reflectances arising from surface scattering. That is to say, the brightness on the radar image will be due foremost to surface scattering of the impinging signal. In general, people refer to this as surface roughness, where roughness is defined in terms of the

wavelength, and which we describe as image tone. Tones on the HV image, in contrast, can be shown to be a function primarily of "volume" scattering. By "volume" we mean to imply that signals are able to penetrate to some depth within the imaged scene. The relative ability of signals to penetrate depends on their polarization, and it turns out that the cross-polarized component (HV) carries most of the information on volume scattering. Therefore, the brighter the return on HV imagery, all other factors being equal, the greater the contribution from volume scattering and, by implication, the more heterogeneous the imaged material. For homogeneous media, there should be little difference between HH and HV reflectances, whereas for heterogeneous media, there should be some contribution to the HV signal.

The fir forest on figure 2-12 has a decidedly darker tone than either of the other two types (both on the HH and HV image).

Relative to the other types, it would appear that fir forest is neither a good surface scatterer (HH



2-12 K-Band radar images of vegetation (left-HH, right-HV). A. White fir forest (*Abies*); B. Ponderosa pine forest (*Pinus*); C. Chaparral shrub (*Arctostaphylos*); D. Area of slope ambiguity. Courtesy Stanley Morain.

polarization) nor a good volume scatterer (HV polarization), since this type is comparatively dark on both images. The reasons behind the darker tone of fir forest are not immediately clear. Part of the explanation may be related to the vertical orientation of the short needles. With such dense, vertically oriented needles, surface scatter may be significantly less than for surrounding vegetation types, leading to a relatively darker tone.

These few examples by no means exhaust the considerations necessary to adequately interpret radar imagery. They are intended only as an introduction to the lines of reasoning that can be employed to extract at least preliminary information and to explain the appearance of selected phenomena. There is need, still, to consider the interactions of moisture and viewing angle with different scene compositions and roughnesses in order to fully understand the value of this form of imaging system.

Applications in Archeology. Despite the vast and rapidly growing literature on radar applications listed by Bryan (1973), there are virtually no reports describing archeological results per se. There are, however, definite areas of application which should be explored. These would include detection of occupation sites, lineament analysis for ancient road and irrigation nets, detection of subsurface structures, and mapping of regrowth in previously cleared areas. For these possibilities there are ample research results to suggest a pay-off in archeology. The sensitivity of radar systems to reflections from vertical structures (surface and to some extent subsurface), to moisture patterns in soil and along lineations, and to changes in vegetation structure and physiognomy have all been documented for environments ranging from the tropics to polar latitudes. Figure 2-13 shows examples of several terrain situations that may have value in archeological research.

Though preliminary in scope, considerable research has been reported on radar reflections from cultural settings (Lewis, et al., 1969). The important attributes governing reflection are building material, the diplanes and tri-corner vertices formed by walls, and the height and density of buildings. For location of low level archeological structures molded from local building materials like adobe or mud, the most important of these attributes would probably be the diplanes and tri-corner vertices. Quarried building materials, typical of more advanced civilizations, might be more easily distinguishable from surround-

ing targets than adobe, especially if the walls are still intact and not covered by vegetation.

The detection of vegetation patterns associated with formerly cleared agricultural sites is readily detectable in forested areas, as shown in figure 2-13. Here the important factor is the height difference between formerly cleared areas and mature forest. When imaged at high oblique angles by radar, rather subtle differences can be mapped. Interpretations would probably not lead in most instances to immediate archeological discoveries, but might serve the time-saving role of deciding where further field investigations should be initiated.

Passive Microwave Sensors

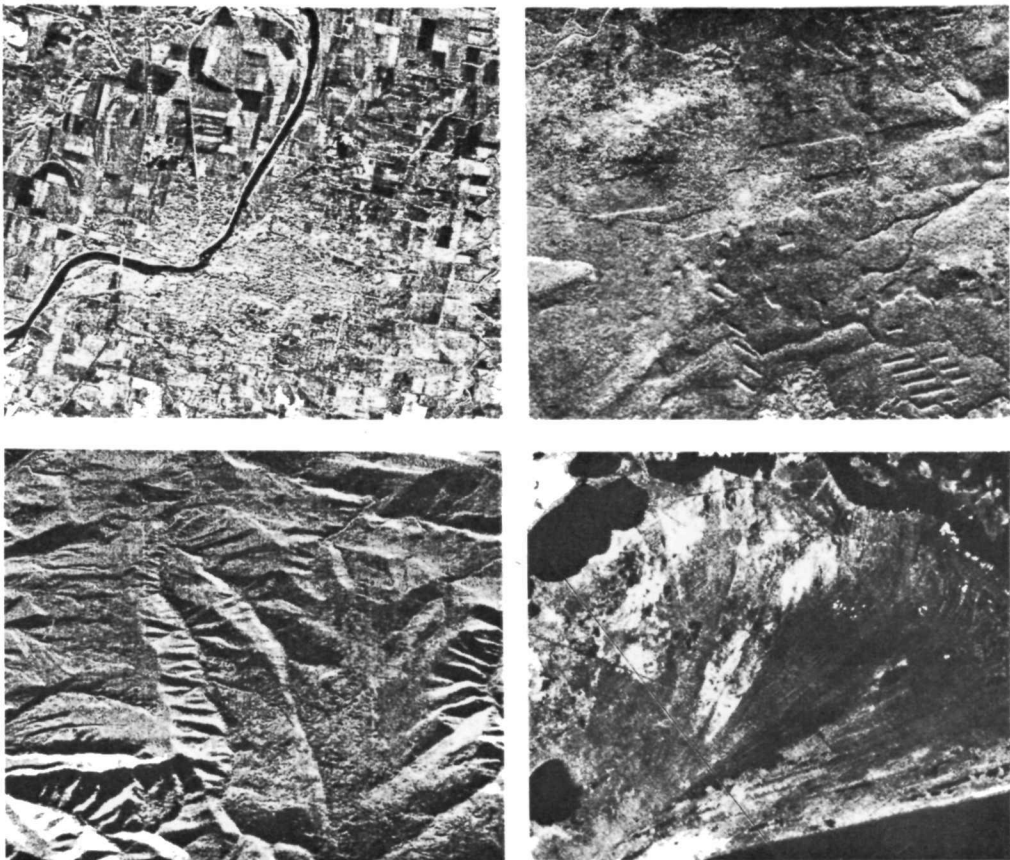
Sensor Operation. Passive microwave radiometers operate in the 1 mm. to 1 m. wavelength region. Wien's Displacement Law teaches us that power radiated at these wavelengths is rather small. Nevertheless, there is measurable radiation, and the detection and measurement of it for certain terrain, atmospheric, and oceanographic analyses has proven useful. We speak of "passive" microwave in this section in order to distinguish both the sensor operation and its applications from "active" microwave sensors (radar). Passive sensors record naturally emitted, reflected, and transmitted radiation, whereas the active sensors illuminate the terrain by transmitting a signal of known wavelength and recording the amount of reflection or "backscatter".

All natural objects emit radiation in the millimeter wavelength range, the amount of which is temperature dependent just as it is in the thermal region. At those longer wavelengths, there is little atmospheric absorption except for narrow water and oxygen bands around 1 cm. There is, however, considerable atmospheric scattering and self emission, and this contributes to a "noisy" environment for sensor operation. Because the total quantity of microwave radiation is small, sensors must be designed to amplify many times the energy received at the antenna. This, of course, means that spaceborne radiometers in particular have poorer spatial resolution (on the order of several kilometers) as a trade-off for finer spectral resolution. Airborne sensors achieve usable resolutions because the antenna beam width subtends a smaller area on the ground at lower elevations.

Image microwave radiometers function through the use of a fixed antenna that receives but does not

2-13

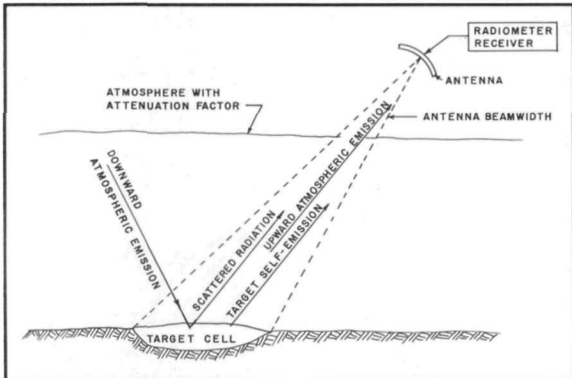
Radar imagery of varying terrain features. Clockwise from the upper left: City of Lawrence, Kansas showing urban built-up area surrounded by several types of agricultural land; forested area showing zones of clear-cutting; marshland area showing varying concentrations of soil moisture — the light areas have a high concentration of moisture while the darker areas have a lower concentration; mountainous terrain showing the reflectance characteristics of several slope angles and forest types. Courtesy University of Kansas, Center for Research, Inc.



transmit emitted energy of a given wavelength. The forward motion of the platform provides the means whereby a strip image can be produced. The general configuration of a radiometer and the factors affecting received radiation are shown in figure 2-14.

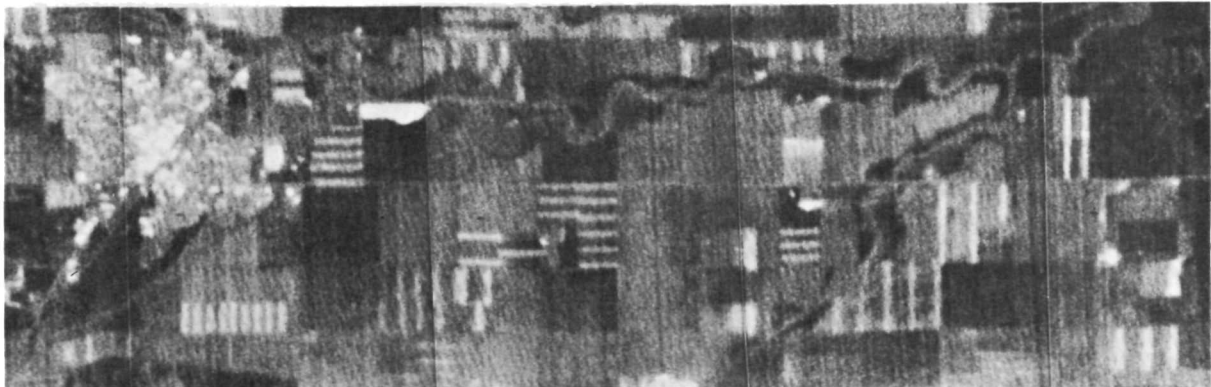
Basic Image Interpretation. Passive microwave radiometers record a parameter referred to as "brightness temperature". At millimeter and centimeter wavelengths, the amount of emitted radiation is so small that the earth appears to be exceedingly cold, well below 0°C (273°K). Obviously, terrain features over most of the globe are well above 0°C so with passive microwave radiometers, we are recording an "apparent temperature" or, as it is more widely known, a "brightness temperature." This value, however, is recorded by an antenna having a fixed viewing angle and azimuth angle with respect to the ground. Since few, if any, objects in nature are iso-emissive or iso-reflective, we can be certain that the apparent temperature will vary as a

function of these angles as well as from signal polarization and atmospheric conditions. In the absence of complete angular information about a given target and because any given resolution cell may have radiation contributions from a number of elements, the observed brightness temperature is best expressed in terms of a black body equivalent. That is, the power radiated by a resolution cell on the ground (a "grey" body having imperfect radiation) has the same brightness temperature as a black body (an ideally perfect radiator) having a lower temperature. The brightness temperature for each resolution cell is recorded on strip images as shades of grey. Lighter image tones are interpreted as colder (lower microwave radiation); darker tones as warmer. Figure 2-15 is a microwave radiometer (MICRAD) image obtained in 1974 over Coalinga, California. This scene was imaged June 26, 1974 by the China Lake Naval Weapons Center's passive microwave system at an altitude of 6,500 feet above the terrain. Commercial and industrial features



2-14 Configuration of a radiometer and factors affecting received radiation. *Modified from Manual of Remote Sensing.*

2-15 Microwave radiometer (MICRAD) image of Coalinga, California and surrounding agricultural region. *Courtesy China Lake Naval Weapons Center and University of California at Santa Barbara.*



within the city of Coalinga (upper left) elicit a brighter response than surrounding residential areas. An unpaved road and a few oil sumps (bright spots) are visible in the oil fields (upper right). Irrigation activities are evident in many of the agricultural fields.

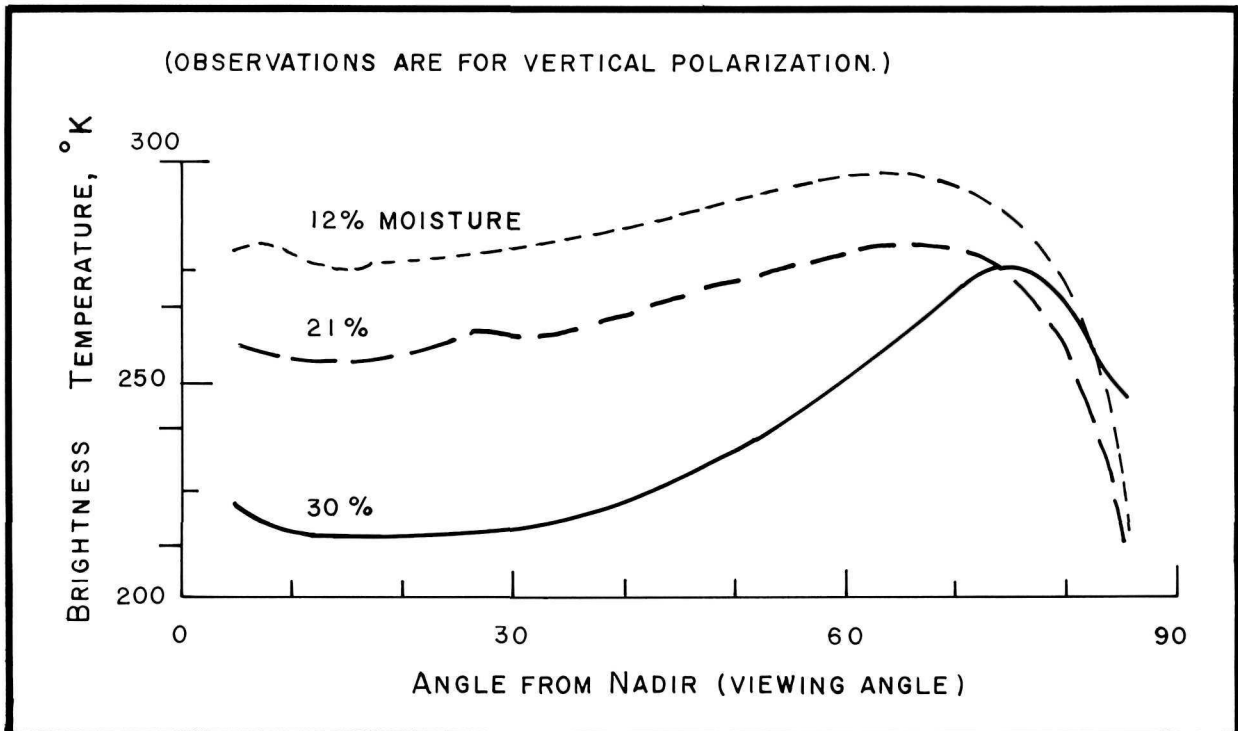
Experiments to date indicate that passive microwave might best be applied to studies in meteorology, oceanography, geology, and soil moisture. The data in figure 2-16 illustrate that there are significant brightness temperature differences for a given soil depending upon its moisture status. These differences are seen over a wide range of antenna viewing angles but are often most pronounced between the nadir (directly beneath the platform) and about 45°.

Broad area studies in meteorology and oceanography are best achieved using satellite platforms.

Satellite imaging of global cloud patterns and high altitude imaging of the land-sea-ice boundaries

in cold climatic regions have seen the most use of passive microwave sensors. Plate 3 shows a color enhanced image of arctic sea ice where brightness temperatures ranging from 190°K to 270°K are shown. Work has also been carried out on the surface conditions of the oceans, or "sea-state". It does not appear, however, that ocean surface temperatures, as such, can be measured from satellites or high-altitude aircraft due to problems incurred from surface roughness (Edgerton and Trexler, 1973).

Applications in Archeology. The best application of passive microwave sensing in archeology appears to lie in soil moisture evaluations. This characteristic could lead to the discovery of buried ditches and other man-made phenomena which cause variations in soil moisture. Beyond this very simple statement, there are virtually no experimental or empirical results upon which to base an adequate archeological assessment.



2-16 Diagram illustrating the effect of soil moisture on brightness temperature. Source: Kennedy, Edgerton and Sakamoto, 1966.

Ground-Based Instrumentation

Remote sensing is not restricted to space or airborne sensors. The definition of remote sensing is “the detection and measurement of distant objects without coming into contact with those objects”. In archeology, we take considerable interest in buried structures and artifacts, objects that are not visible to the eye and quite probably not directly detectable using space or airborne sensors. This is the area in which ground based remote sensing plays a vital role. With devices such as magnetometers, resistivity meters, ground-based radar, and water-borne sonar, we are able to save time and energy in the search for antiquities by knowing where and how deep to dig.

Magnetometers, resistivity meters, and truck mounted radars are generally used at known archeological sites since their lack of mobility and small sensing ranges make them impractical for searches over uncharted areas. Cesium and proton

magnetometers measure the magnetic characteristics of the top several meters of the earth's surface. Buried structures and artifacts quite often have different magnetic properties than the surrounding soil, especially if they were heated at some time during their manufacture. These differences are often identifiable on a magnetometer readout (fig. 2-17).

Resistivity meters record the flow of electric current through the ground. Buried objects will often impede or alter these currents and these can be detected and located. Ground-based radar works on the same time-delayed echo principle as was described earlier. Buried objects and structures are often identified by peaks and valleys plotted on the radar profile.

When an archeological site has been pinpointed for investigation, it is general practice to plot a grid system over which the instrument scans will be made. The size of the grid depends on the total area to be investigated, the amount of time available, and the sensitivity of the instrument. The

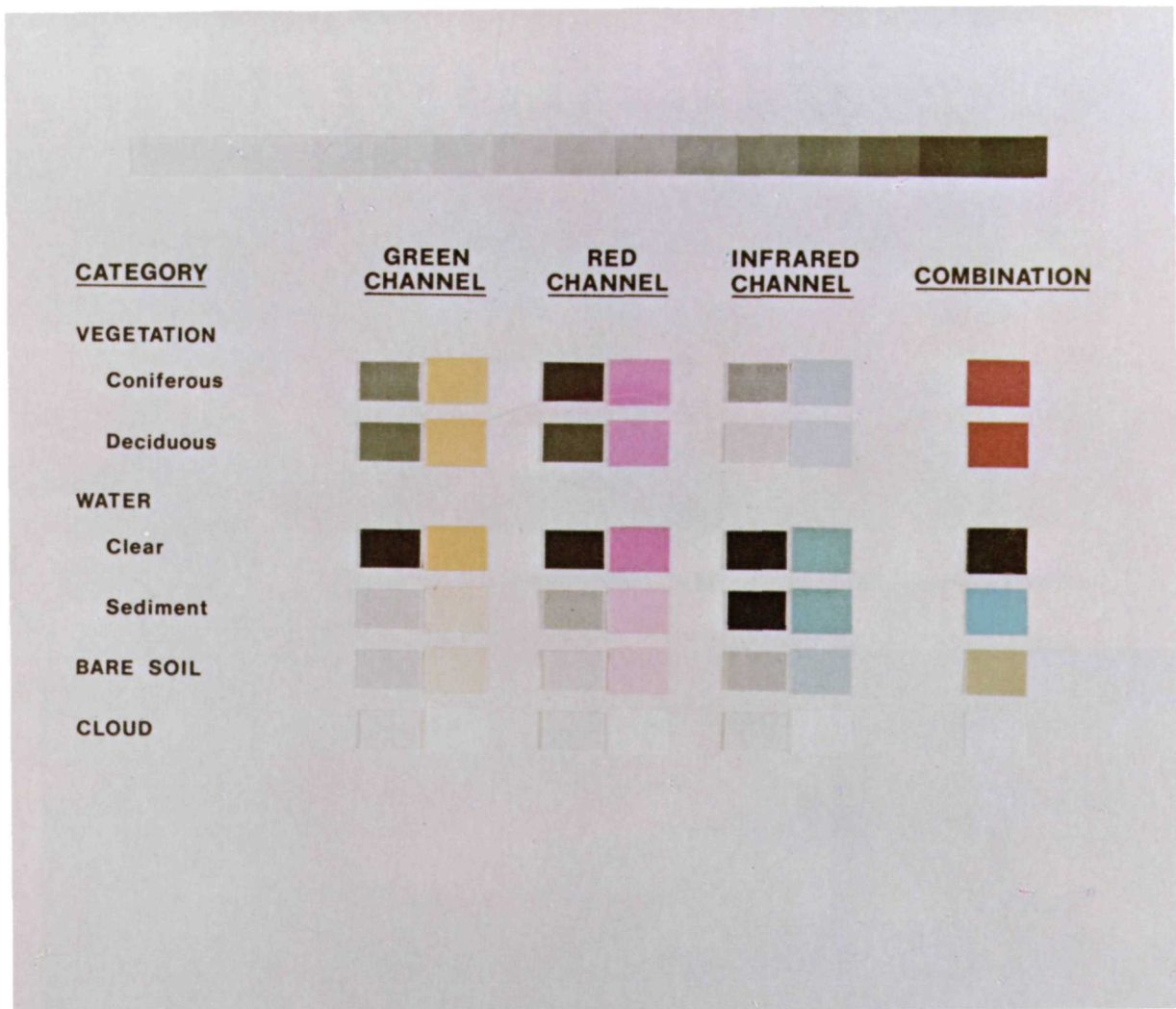


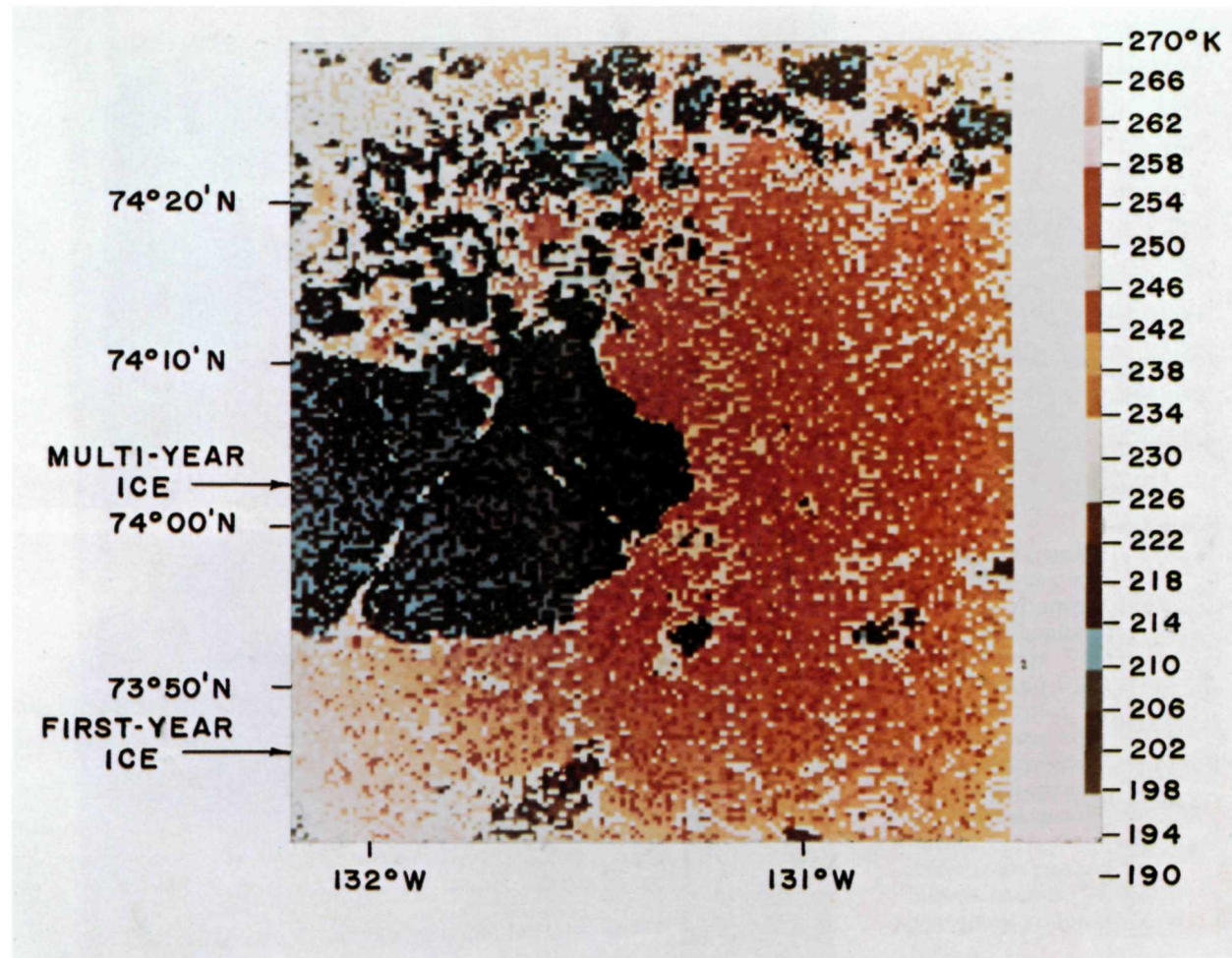
Plate 1 Chart demonstrating essential points of Landsat interpretation. Courtesy Technology Application Center.

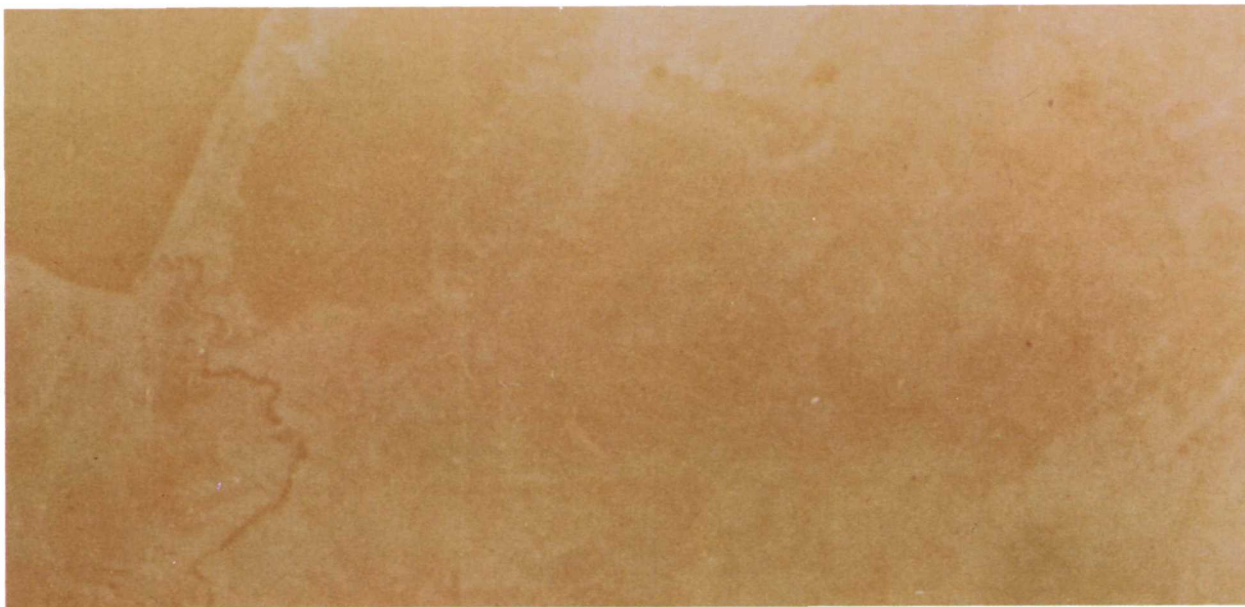


Plate 2

Landsat image of a portion of the Rio Grande Valley of New Mexico.
Courtesy Technology Application Center.

Plate 3
A color enhanced
passive microwave
image of arctic sea
ice. *Source: Technology Reports Center*

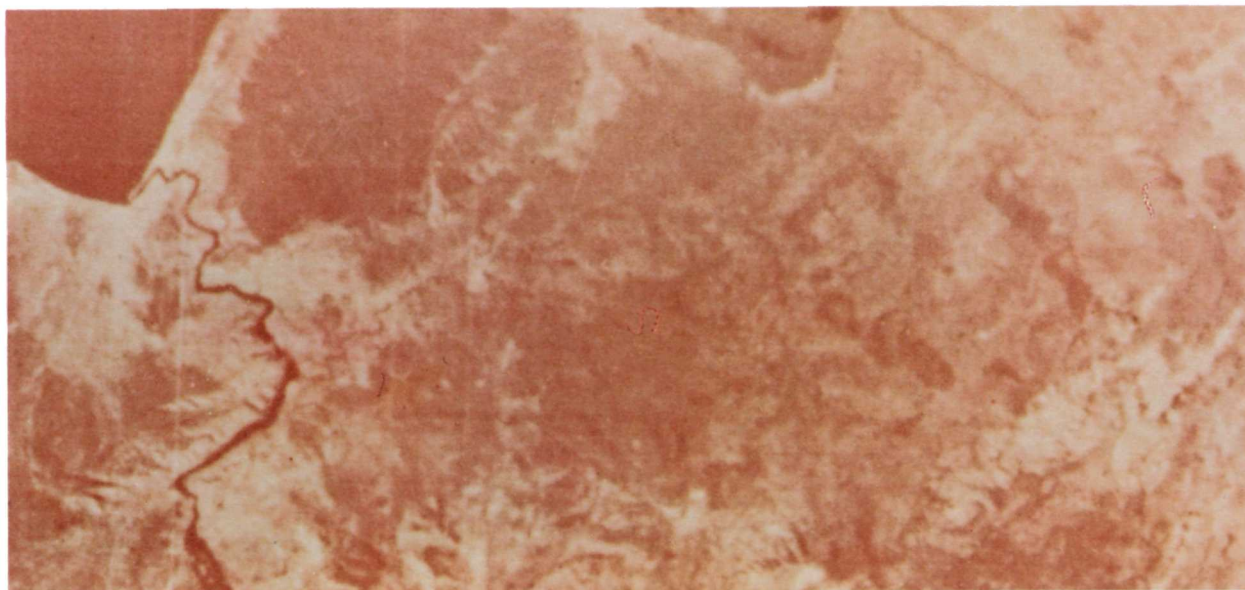


**Plate 4**

The diazochrome process demonstrated on a Landsat image:

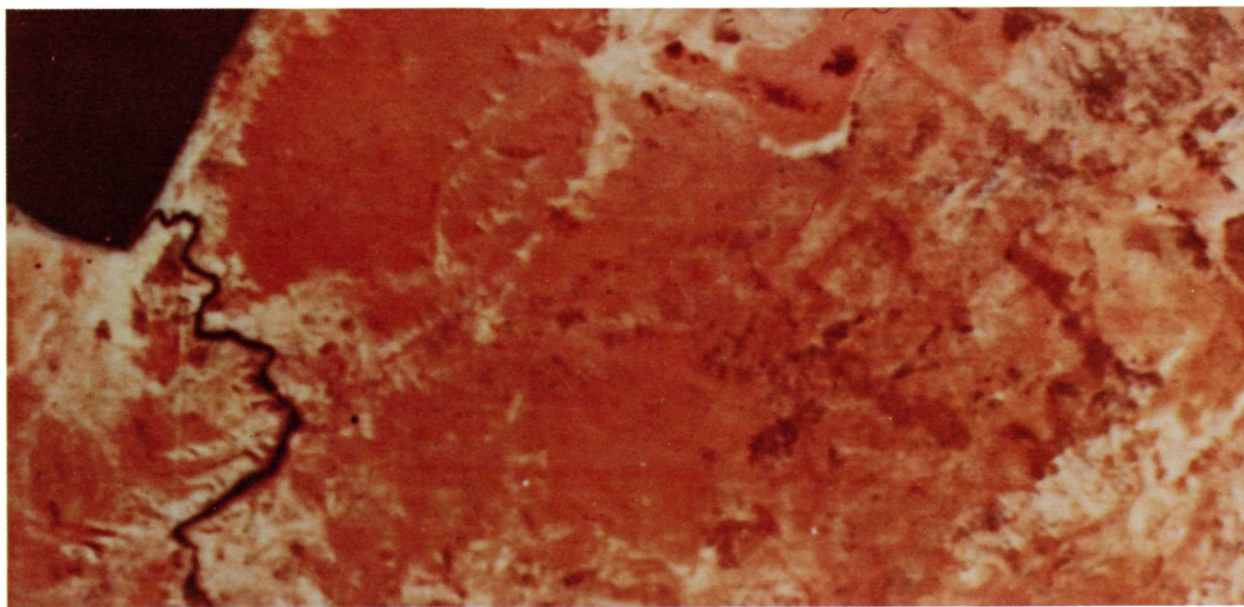
- A. Yellow sheet (green channel)
- B. Magenta sheet (red channel)
- C. Cyan sheet (infrared channel)
- D. Color composite of A, B, and C

Courtesy Technology Application Center

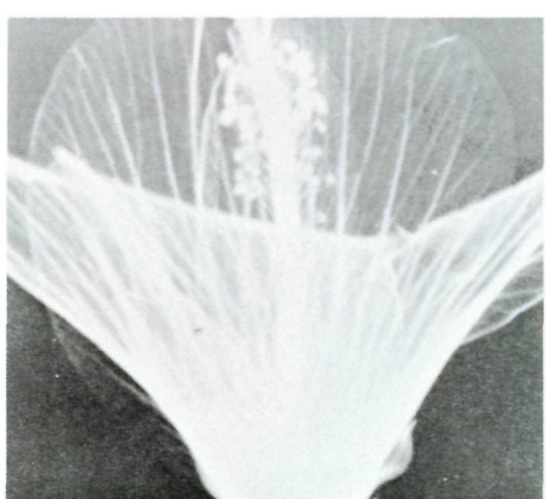
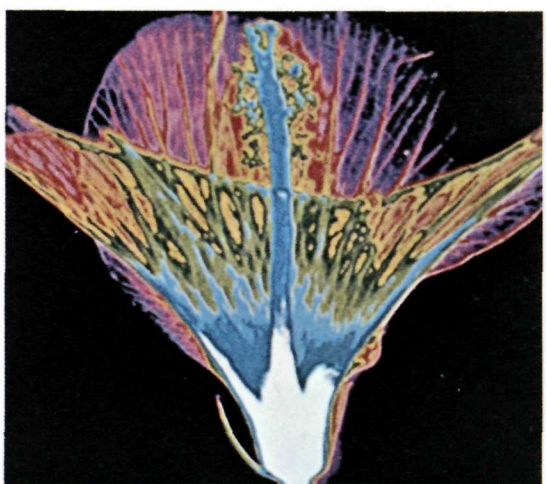
**B**



C

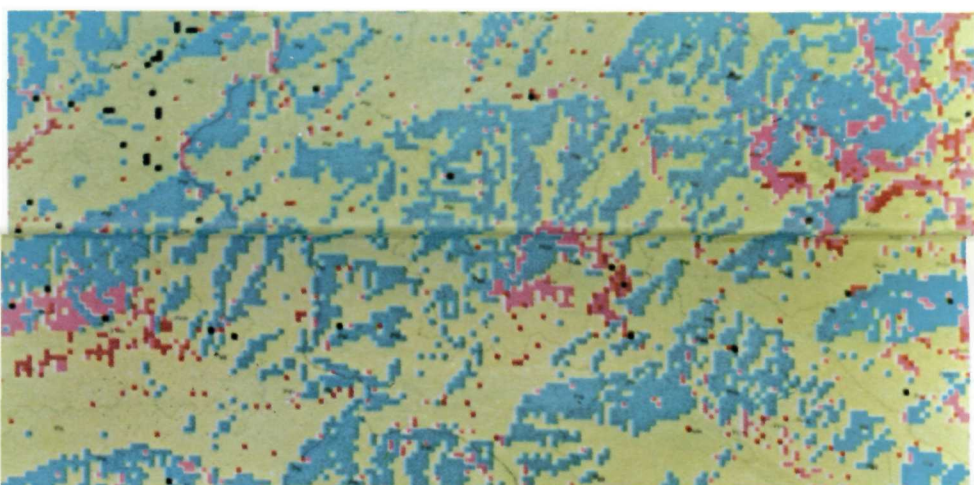
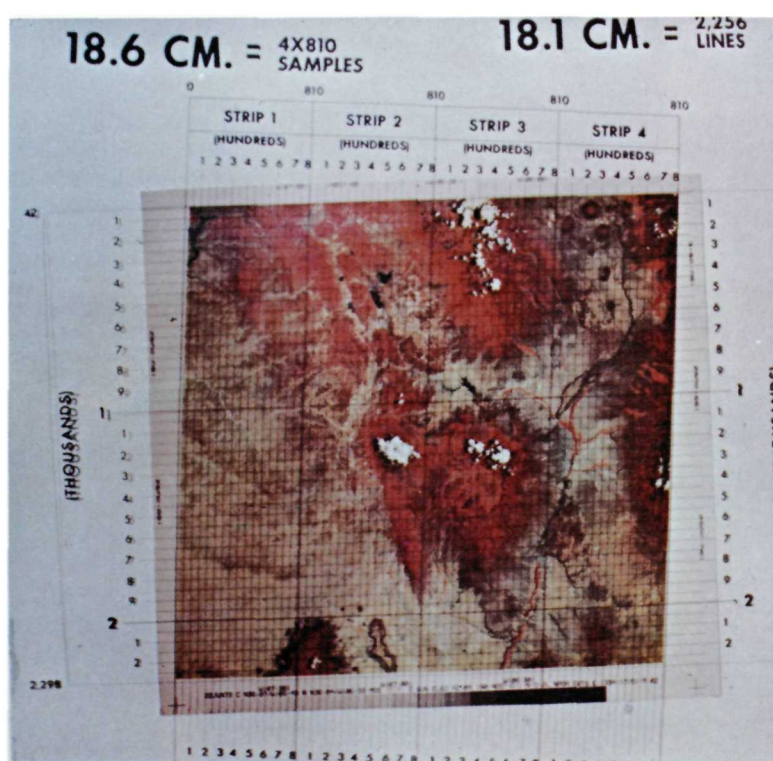
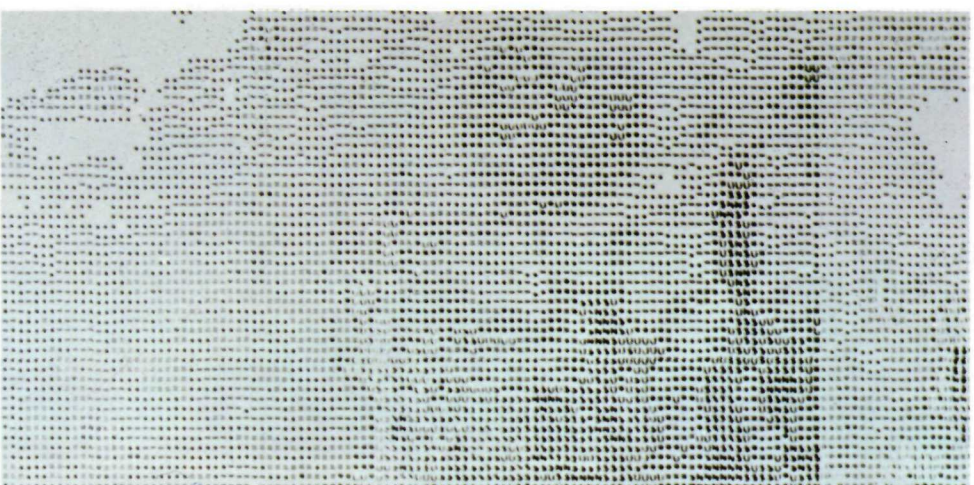


D

**A****B****C****Plate 5**

- Closed circuit television techniques:
 A. Standard black-and-white image
 B. Color enhancement of A
 C. Edge enhancement of A
Courtesy Spatial Data Systems, Inc.

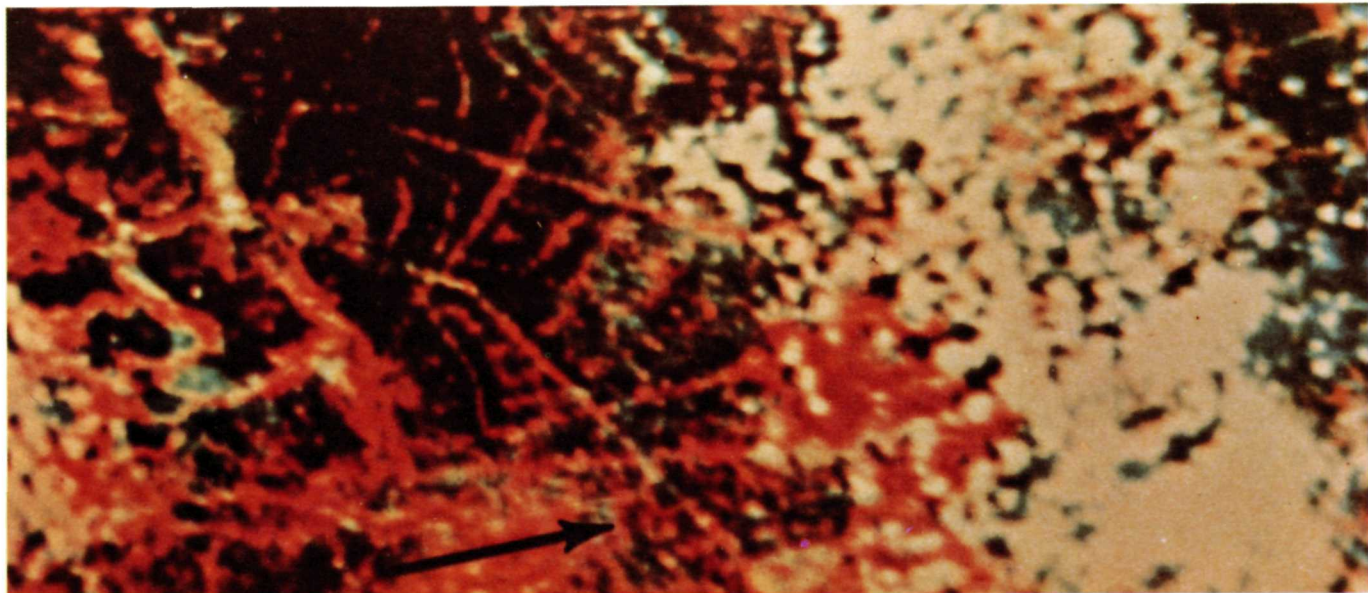
Plate 7
 Demonstration of the use of pixel overlays to aid in precise coordinate location on Landsat images. *Courtesy Technology Application Center.*

**A****B****Plate 6**

- Digital image output formats:
 A. Color television display
 B. Computer printout
 C. Color computer printout

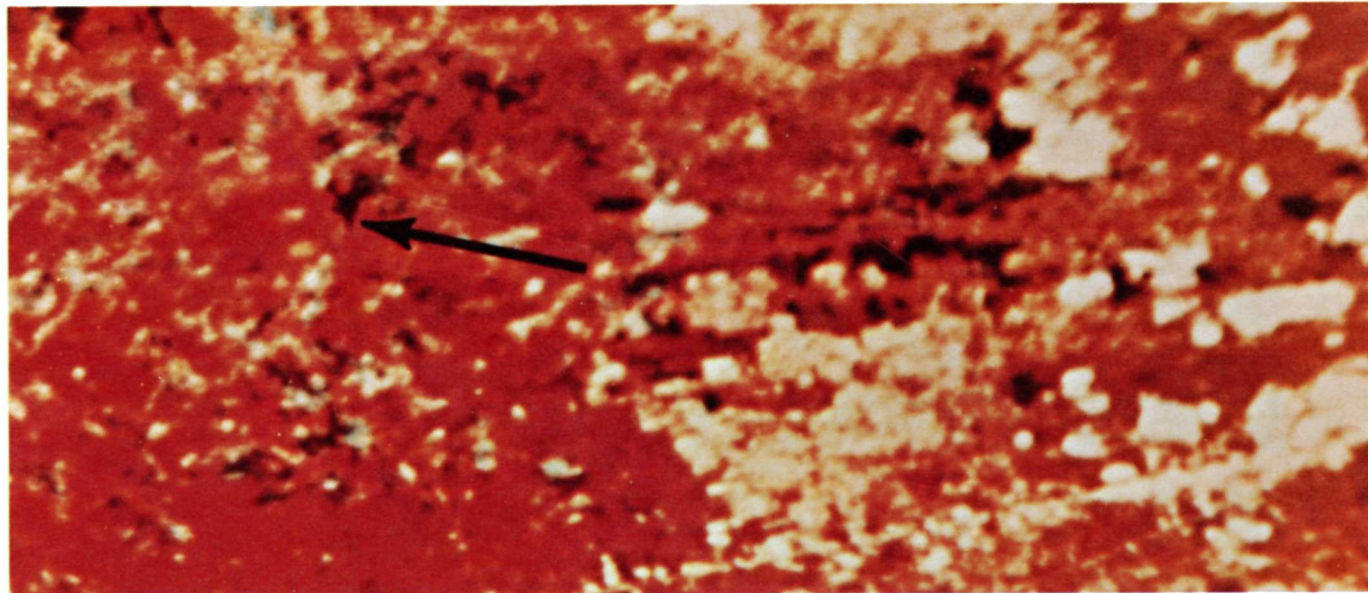
Courtesy (A) U.S. Geological Survey; (B) Technology Application Center; (C) Colorado State University.

**C**

**Plate 8**

Example of scale adjustments using Landsat digital tapes. A shows every fourth line and every fourth sample and is at a scale of 1:1,000,000. The scale increases through D which is at a scale of 1:24,000 and displays all pixels. The arrows point to a temple complex near Bangkok, Thailand. The temple is indicated by the blue and white pixels clustered together inside the moat on the right side.

Courtesy LARS (*Laboratory for Applications of Remote Sensing*). **B**



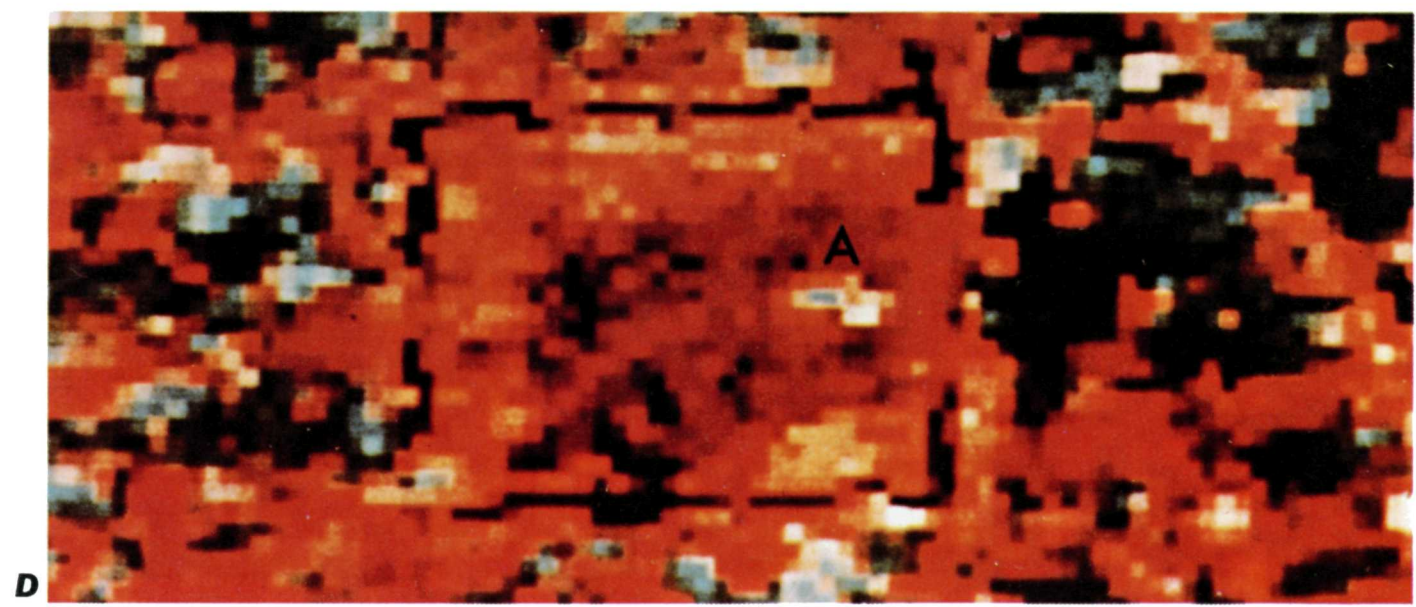
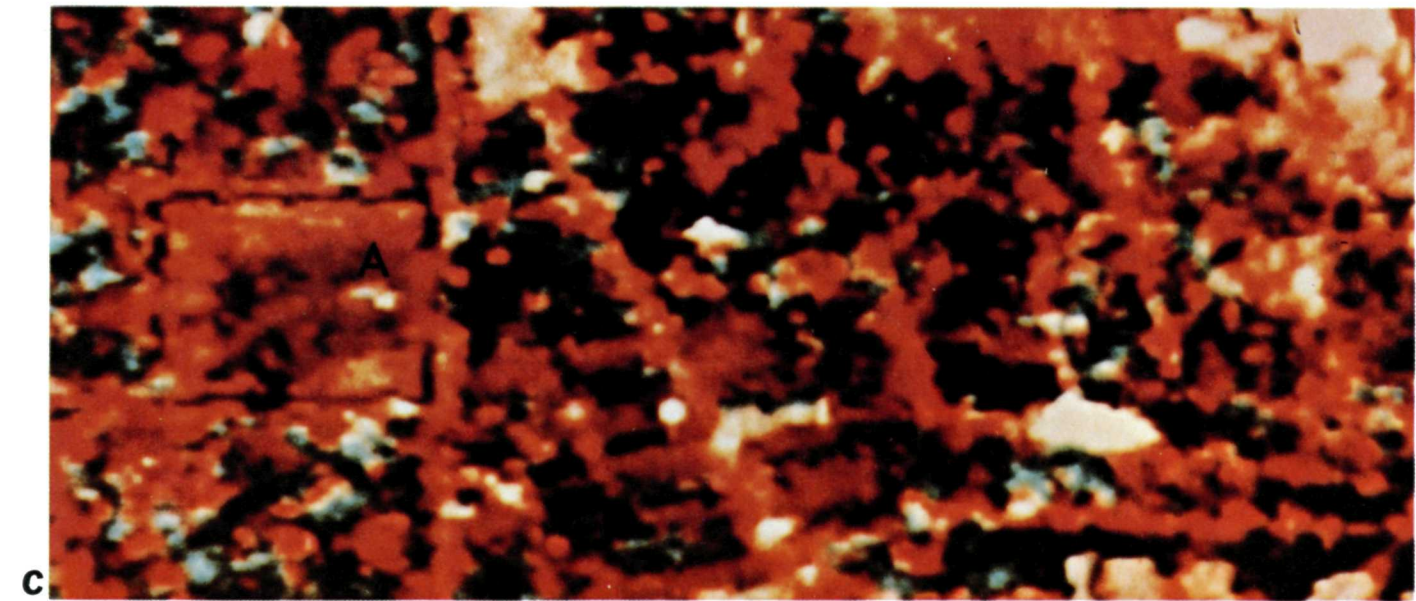
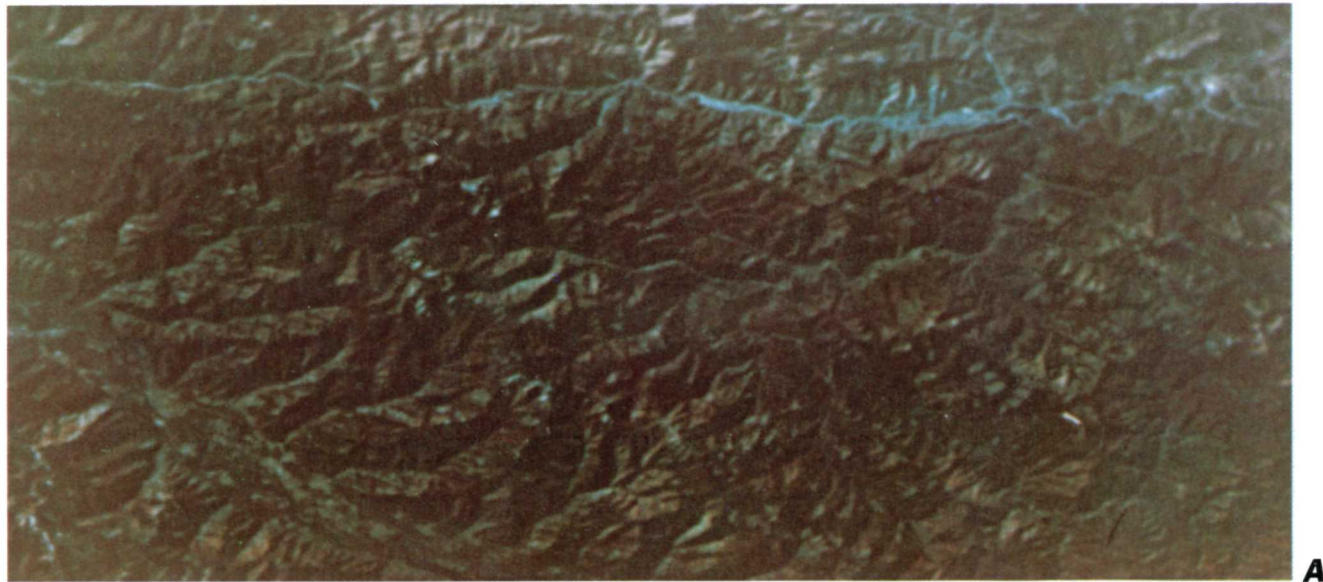


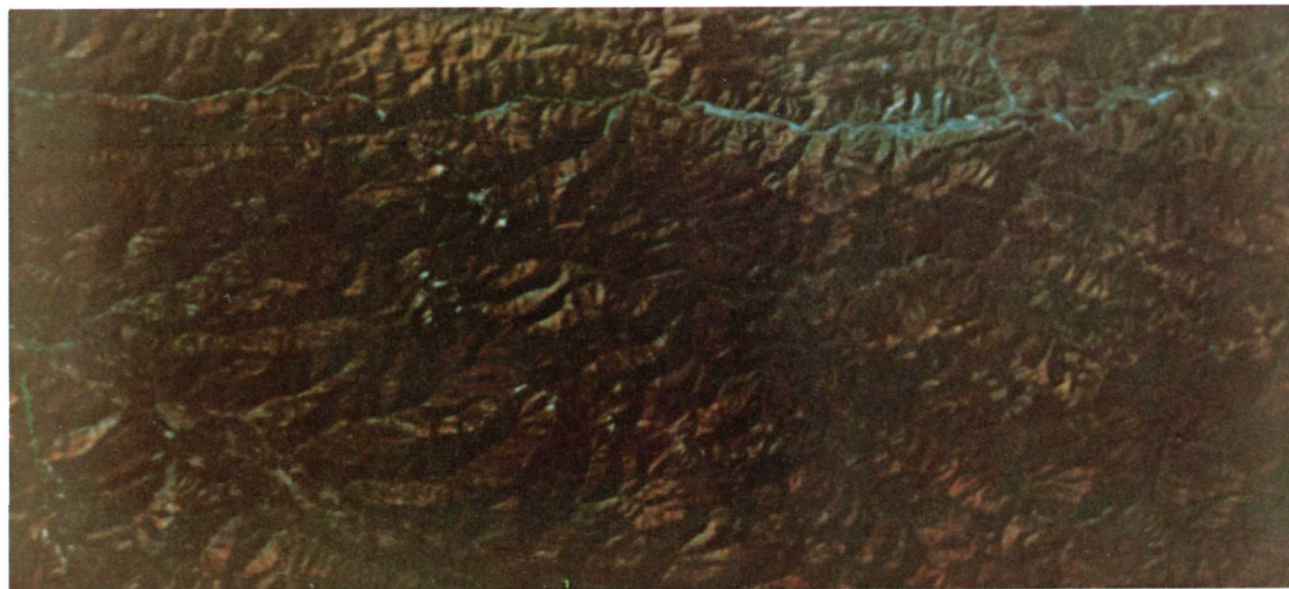
Plate 9

Examples of Landsat image corrections:

- A. No corrections
- B. Haze correction
- C. Solar elevation correction

Courtesy Chavez, 1975





B



C

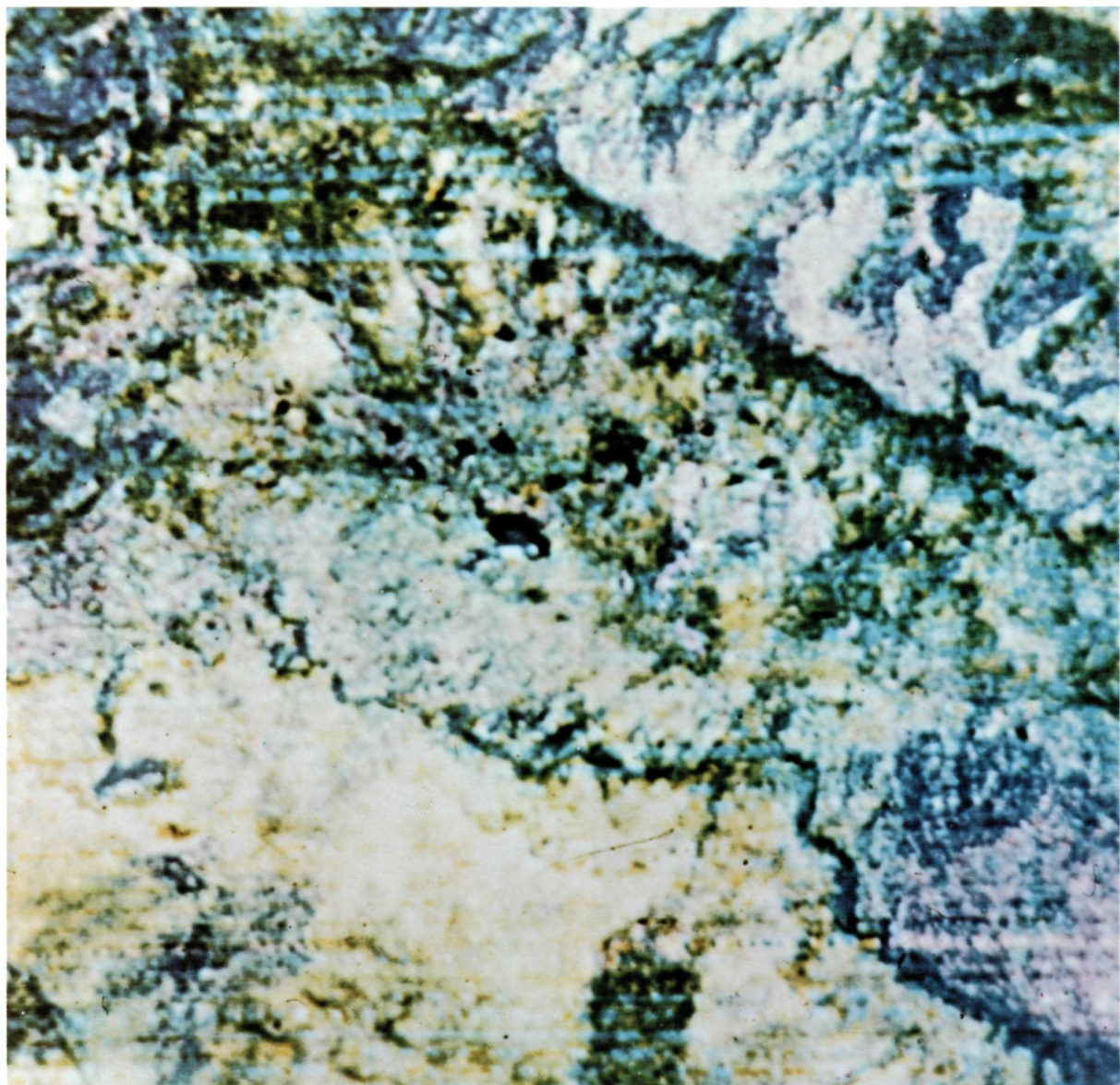


Plate 10 Example of band ratioing of a Landsat image. The green/red ratio is displayed in green; the green/infrared (700-800nm) ratio is displayed in red; and the green/infrared (800-1100nm) ratio is displayed in blue. *Courtesy Los Alamos Scientific Laboratory and the New Mexico Bureau of Mines.*

grid also serves as an excellent control for making detailed maps of the site.

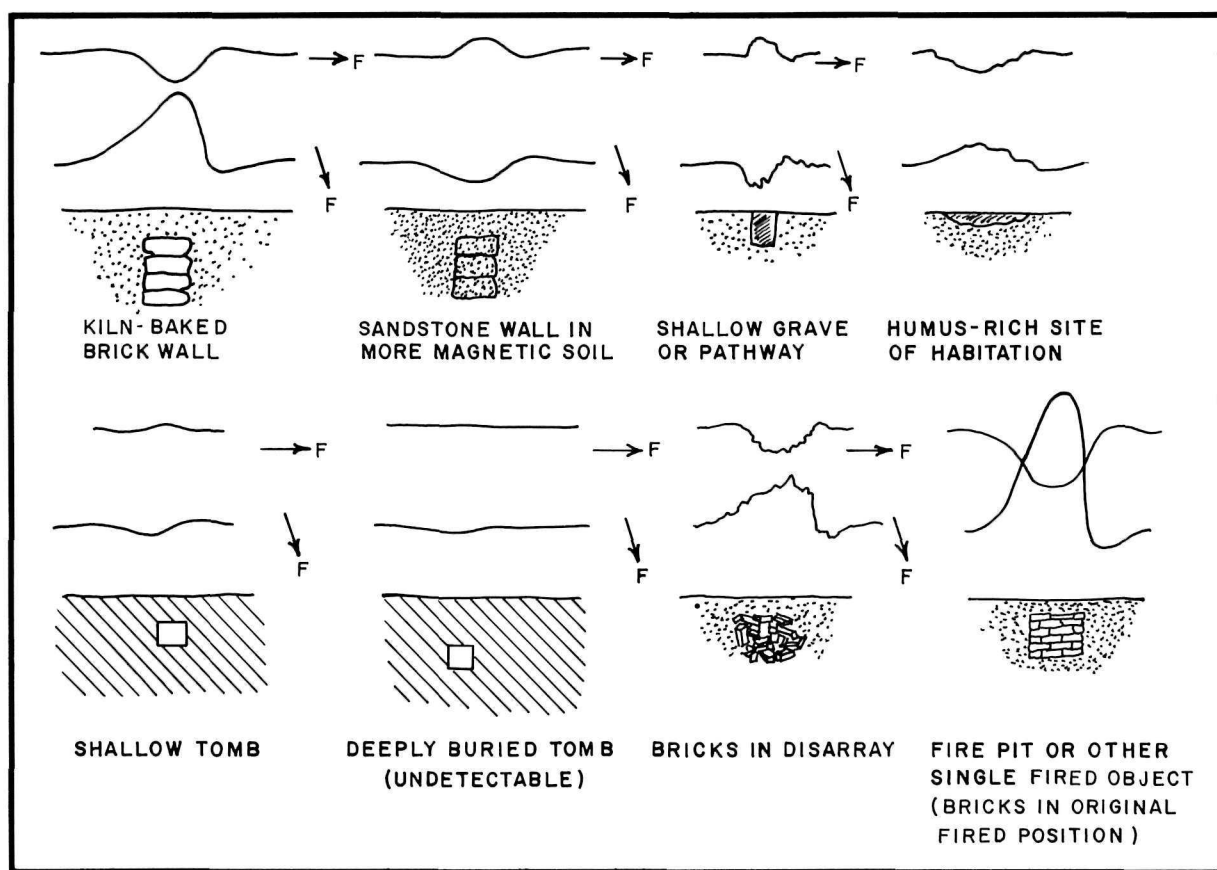
Before measurements are begun, it is common practice to make several test measurements of areas which are similar in soil type and conditions as the excavation site but which do not have suspected anomalies. This is important because the basic characteristics of the soil must be known so that any anomalous features will be detected.

Anomalies exist at archeological sites because of the contrast in magnetic properties between cultural features or artifacts and the surrounding medium, be it soil, rock or empty space. Remanent magnetization is usually present in objects which have undergone heating sometime in their history and is the cause of most magnetic anomalies arising from cultural features.

Remanent magnetization is created when clays or soils with a high magnetite content are heated to relatively high temperatures and then cooled in the presence of the earth's magnetic field. Upon cooling, the magnetite crystals move and eventually align themselves with the earth's magnetic field and parallel to each other, thus creating a magnetization fixed with respect to the object and parallel to the earth's total field at the time of cooling (Breiner, 1973).

It is the presence of these magnetic fields which are searched for at archeological sites. Objects which could possess magnetic fields of this type of origin are mud brick walls, pottery, tiles, etc., (fig. 2-17).

Underwater archeology has taken great strides in recent years as technology has improved. It would be ideal, of course, if underwater archeology could



2-17 Examples of buried cultural features and how their magnetic anomalies could appear. "F" indicates inclination of magnetic field when the profiles are taken in different directions. Source: Breiner, 1973.

be done in shallow clear water with the unaided eye or by underwater television cameras. In practice, however, most shipwrecks seem to occur in deep, murky water in which simply locating the wreck may be as difficult a problem as excavating it. Side scanning sonars have proved to be effective in searching large areas in a short period of time. They are effective in mapping the ocean bottoms and locating wrecks. Shortpulse sonars have located wrecks several meters beneath the ocean bottom.

Section 3

Image and Data Processing

The techniques for processing imagery and digital data obtained by various remote sensors can be grouped under two headings: analog and digital. Analog processing includes image projection through filters and color enhancement (film density "slicing") on closed-circuit TV. In these circumstances, film densities control the proportion of light transmitted through the colored filter or are converted to equivalent voltages and used as input to the color guns of a TV system. At no point, either in the input or output stages of the analysis, are any quantitative digital values employed.

In digital analysis, on the other hand, film densities may be converted into numerical form for statistical or computer analysis. Prior to the advent of multispectral scanners, almost all digital data were obtained by densitometry from image transparencies; more modern systems record the data immediately into digital format for later conversion into images.

Analog Processing Techniques

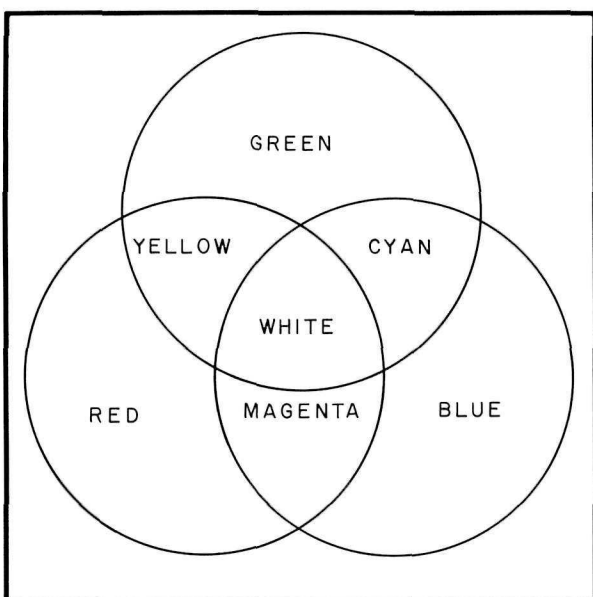
Once an aerial or satellite image is in hand, there are a number of methods by which it can be altered to aid interpretation. One of these methods is with a color additive viewer; another is through the use of diazochrome material. Before a discussion is undertaken of either of these, it is necessary to review what is meant by "color".

Color can be formed by two processes—addition or subtraction. All photographic processes and, indeed, all color in nature is seen because of subtractive processes. Once white light has been partitioned into its component wavelengths, as by passing it through a prism, the color we see is a result of the absence or absorption of all other wavelengths.

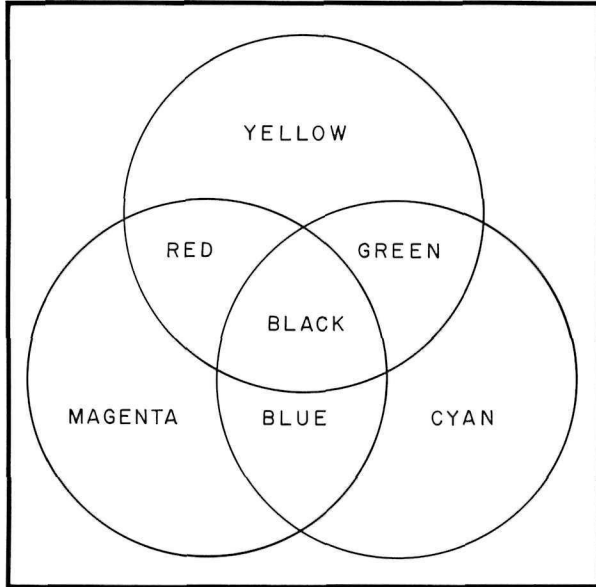
In additive color formation, which can only be done with light sources, there are three primary

colors: red, green and blue. By mixing various proportions of these additive "primaries", almost all conceivable colors can be formed on a screen. Figure 3-1 shows that red and green light combine to form yellow, blue combined with green forms cyan, and red with blue forms magenta. The mixture of all three primaries produces "white" light. The additive process is dependent upon the fact that each primary must be projected on a common screen.

In subtractive color formation, which includes all photographic darkroom processes, there are also three primaries: cyan, magenta and yellow. The recombination of these colors produces black instead of white. Paired combinations will generate the additive primaries but do so through a subtractive process. Figure 3-2 shows the relationships of the subtractive primaries.



3-1 Color additive process. Source: Scherz and Stevens, 1970.



3-2 Color subtractive process. Source: Scherz and Stevens, 1970.

Color Additive Viewer. A color additive viewer is used to make false color combinations by placing black and white 70mm transparencies (either positives or negatives) of up to 4 separate channels into a mounting board. The board is then placed into the viewer with each transparency in front of a light source. In front of each transparency is a set of interchangeable colored filters, usually mounted on a rotating wheel. Some or all of the transparencies can be superimposed onto a common screen at the same time and different combinations of filters may be applied to enhance tone contrast or color differences on the composite image. Micro adjustments are provided for precise registration of the images.

In the color additive viewer, color is formed by an additive process because blue, red and green light are superimposed to form white. For example, consider the appearance of a cloud on the green, red and infrared transparencies of a Landsat scene. The film density for the cloud area will be very low (the film will be almost perfectly transparent). The cloud area will appear this way on all three images. Therefore, if the green channel image is projected through a green filter, the purest or most intense shade of green will appear over the cloud area. The same argument will hold for the other two images and their respective filters. The result will be a white cloud on the composite and it will have been generated by the addition of red, green and blue light.

In practice, the color additive viewer has been most useful in generating false color composites. Its main drawback is that we have no *a priori* knowledge of which spectral regions and filter combinations will best display desired information. Considerable amounts of time can be spent registering images and creating composites which, in the final analysis, enhance little of interest. On the other hand, hours of patient experimentation (trial and error) can be suddenly rewarding with the appearance of a long sought after subtle archeological feature.

Diazochrome Color Composites. This process differs from the color additive viewer in that it does not use filtered light. Instead, positive transparencies, usually in 9 by 9 in. (228 mm^2) format, are used in conjunction with an ultraviolet light source to expose diazo material to thereby remove color from its surface. To create a false color composite from Landsat images, the green channel is used to expose a yellow diazo sheet; the red channel exposes magenta; and the infrared exposes cyan.

Wherever the transparencies have low film density, as over clouds, more color is removed during the exposure. The darker the areas, the more color will remain. In other words, the color forming process is exactly the opposite from that described for the color additive view. Typical results follow the pattern illustrated in Plate 4.

Closed Circuit Television Systems. Closed circuit television systems have greatly increased our ability to analyze and interpret imagery.

The basic format of a closed circuit TV system would include: 1) a color density monitor, 2) an edge enhancer monitor, 3) a television camera, and 4) an illuminating surface or light table. A black and white or color image, either in print or transparency form, is placed on the light table or on a flat surface beneath a vertically oriented television camera. The image is broadcast by the camera onto the television monitor.

The color density slicer is capable of separating the film density range of the image into as many as 32 or even 64 steps (depending on brand and model) and assigning a color to each. An example of this color assignment or "enhancement" is shown in Plate 5B. The color divisions can be combined, taken out, or reassigned to reveal the desired vegetation, soil or other image patterns. Density slicing helps to highlight the contrast between image tones beyond the normal ability of our eyes.

The edge enhancing monitor contrasts the edges or borders between regions of differing film density. In mathematical terms, the first derivative of the image is constructed and displayed on a television screen. Black lines are produced on the image where the contrast changes from a lighter density to a darker density. This is illustrated in Plate 5C. Conversely, a white line is produced where the image normally changes from darker to lighter. All bright and dark areas on the image are suppressed to the same shade of background gray to further highlight the edges. The density contrast changes are usually made from the left hand to the right hand side of the television monitor.

Edge enhancement has been used in several remote sensing applications. Structural geologists have used the technique to highlight subtle fracture and fault zones. Hydrologists have found applications in drainage network analysis and in plotting turbidity and temperature differences in lakes and streams. In archeology, one could anticipate uses in searching for prehistoric roads, field patterns, irrigation ditches or other linear features indicating the former presence of man.

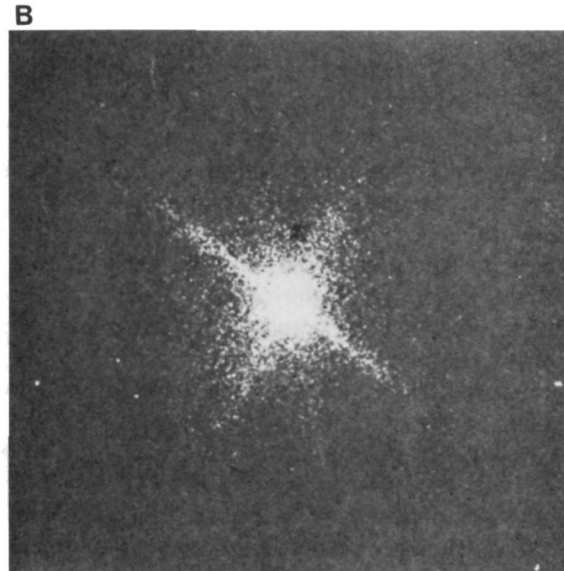
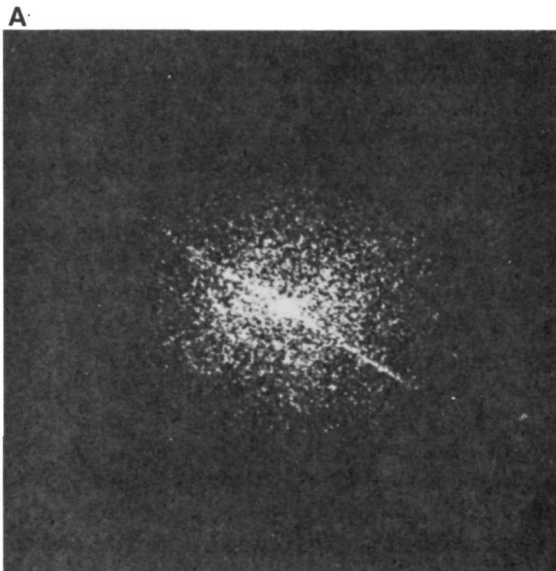
Frequency Transformations. The study of frequency transformations had not been undertaken to any great extent until the introduction of the laser or Light Amplification by Stimulated Emission of Radiation. Lasers are devices that produce coherent

beams of light of the same frequency and wavelength.

Laser image analysis is primarily concerned with detecting patterns and spacings of terrain objects. By projecting laser light through an image and then through one of a large assortment of filters, diffraction gratings, and transforming lenses, a dot pattern is recorded on photographic film. The pattern for these dots is dependent upon the linear and angular orientation of the objects in the image and, in effect, forms a "fingerprint" of what is shown on the image.

Applications of this technique thus far have been in vegetation mapping and surface structure analysis. Hardy (1973) for example, used spatial frequency analysis to investigate the angularities and regularities of vegetation communities at Yellowstone National Park. By taking transparencies of radar and aerial photographic images, he produced laser transforms or Fraunhofer Diffraction Patterns (FDP) of the type shown in figure 3-3.

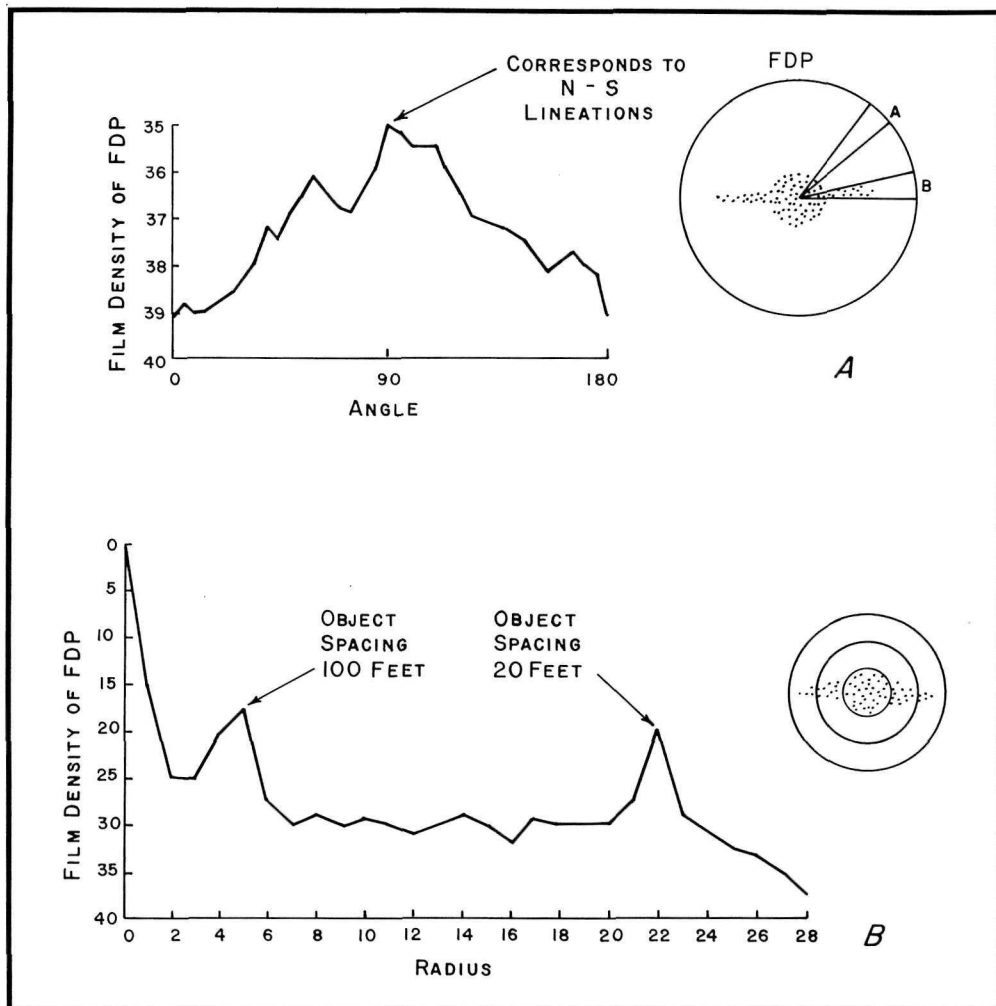
Once such patterns have been produced, they can be analyzed by a process called wedge filtering or annular ring filtering as shown in figure 3-4A. In other words, the FDP can be scrutinized for angular patterns by recording the intensity of light transmitted through a transparency of the FDP over a range from 0° to 180° . Since the FDP is symmetrical about the center point, only 180° needs to be scanned. The process is called wedge filtering



3-3 Filtering of Fraunhofer Diffraction Patterns.

3-4
Example of
Fraunhofer
Diffraction
Patterns (FDP's):
*Modified from
Hardy, 1973.*
Courtesy American
Society of
Photogrammetry.

- A. Wedge filtering
B. Annular ring filtering.



because the angular range over which the light intensity is measured is pie-shaped. In figure 3-4A, for example, the wedge marked B would give a stronger light intensity than the wedge marked A. This would indicate to the interpreter that there were angular relationships on the ground as, for example, street patterns, irrigation networks, etc.

In annular ring filtering (fig. 3-4B), one is interested in determining spacings between objects on the surface. By recording the light transmission in ever increasing rings emanating from the center of an FDP, one can record the presence and magnitude of any such spacings. Peaks in light transmission close to the center of the FDP correspond to large spacings while those farther out correspond to close spacings. The spacings can be calculated precisely if

the scale and resolution of the original imagery are known.

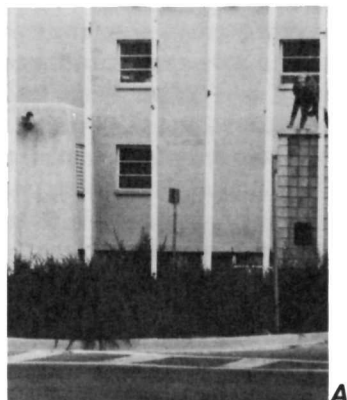
To our knowledge, this image analysis technique has not been used in archeology. Given the quality of modern black and white photography and more recently of narrow bandpass multispectral data, the opportunities for exploring archeological sites in detail from overhead are exciting. Particularly exciting are the prospects for discovering buried phenomena that, through their residual effects, continue to influence surface patterns of moisture or vegetation.

Another method for pinpointing linear features on imagery is the Ronchi ruling. It is an inexpensive and rapid form of wedge filtering. The linear features it can reveal are fault lines, vegetation boun-

daries (as along a fence line), old field patterns, old roads or paths, dikes and ditches, etc. It consists of a sheet of glass or transparent plastic upon which is etched or photographed a series of straight parallel lines. The dark lines and intervening clear areas are of equal width. The rulings are usually manufactured with 200 lines per inch (78 lines per cm) but

other rulings are available with varying densities of lines.

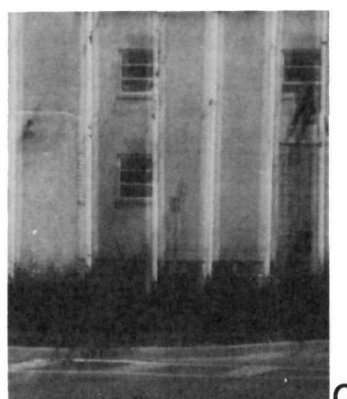
In use, the Ronchi ruling acts as a diffraction grating which, when placed between the observer and an image, enhances some linear image features and blurs or breaks up others depending on the orientation of the ruling. In figure 3-5, for example,



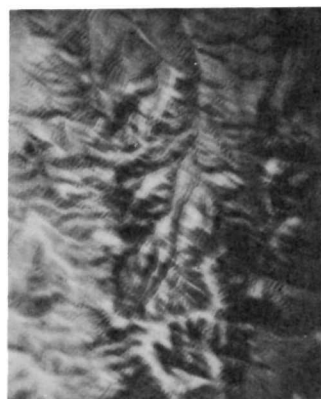
A



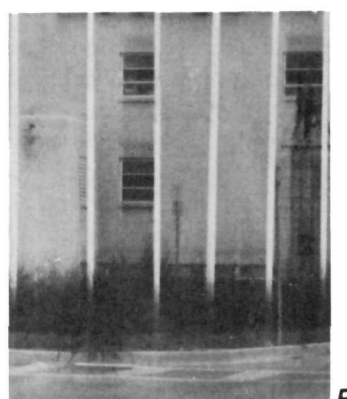
B



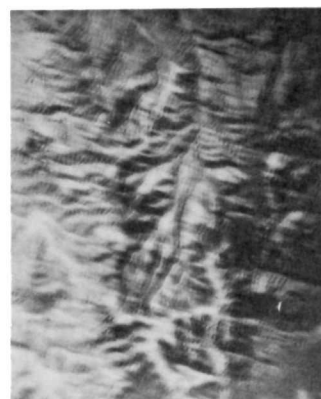
C



D



E



F

3-5

Examples of the use of Ronchi Rulings:

A-B Normal View

C-D Ronchi Ruling turned 90°

E-F Ronchi Ruling turned 180°

Courtesy Technology Application Center.

the image linear features which run parallel to the ruling lines are blurred and the perpendicular ones are enhanced. As the ruling is rotated throughout 180°, different image linear features are enhanced or blacked out. The objective is to reveal linear features which are ordinarily camouflaged among other linear patterns.

The rulings have been most successfully employed in structural geology and glaciology. It has helped to reveal hidden fault lines and fracture zones which, in turn, could indicate areas of mineralization (Offield, 1975). Diffraction gratings similar to the Ronchi ruling have been used with laser light to analyze the snouts of glaciers. They have revealed entirely unsuspected crevasse systems which were actually visible to the unaided eye but were confused by the many criss-crossing fracture systems of the glacier. The rulings have allowed the mapping and measurement of stress and strain angles and have increased knowledge of glacier movement and activity.

In archeology, the rulings could have several useful applications. Linear features such as building foundations, over-grown or buried field patterns, straight sections of old roads, footpaths, and ditches might be enhanced and plotted faster and easier than without the aid of a Ronchi ruling.

Digital Processing Techniques

As stated earlier, these techniques require that image data be available in, or transformable to, numerical format. In this format, the data can be processed automatically or semi-automatically by computer. The field of "pattern recognition" has found wide popularity in remote sensing because of the massive inflow of Landsat digital data. This in turn has stimulated the development of rapid, automatic classification algorithms. The early history of remote sensing literature (that published during the decade of the 1960's) however, describes less sophisticated techniques using line scan and spot densitometers.

Densitometry. Densitometry refers to the quantitative measurement of tonal values of an image. The film density of an image refers to its opacity or transparency measured on a logarithmic scale. For example, an area which is white or light gray is said to have a low film density (positive image); and if it is dark gray to black, it is said to have a high film

density. The density of an image or of objects in it can serve as a parameter for discrimination and identification. Objects which are the same or nearly the same should have nearly the same image density. When viewing an agricultural image, it would be safe to assume that an individual corn field would have nearly the same density as all the other corn fields, but would probably have a different density than wheat or fallow fields.

Densitometers are generally of two basic types—spot densitometers and scanning densitometers. The most up-to-date spot densitometers consist of a "light pencil" or a manually controlled movable light on a television monitor with which certain points on an image may be isolated and measured for density. Scanning densitometers, on the other hand, can make high speed density measurements of entire images and store them on digital tape.

There are two kinds of spot densitometers in common use. One type consists of a light source which transmits light through an image into a photomultiplier tube. The intensity of light is then recorded as a voltage and read-out on a voltmeter. The area whose density is measured is isolated by a disc with a small hole or aperture in it. The disc may be moved over the image in order to pinpoint the precise point desired. Aperture sizes may be varied from 100 microns to 1 mm. It is important to remember that as the aperture size nears the wavelength of the light source, diffraction may occur which would make density measurements meaningless. It should also be remembered that the aperture size becomes the effective resolution element or pixel for the quantized data. No matter what the resolution of the original in-put image might have been, it has been degraded by the aperture.

Another spot densitometer works on the same aperture principle as the one described above but is designed for use with color transparencies. The only additional equipment involved is a four color filter wheel mounted in front of the photo multiplier tube. The colors are red, blue, green and clear. The clear filter may be used to obtain voltage readings in the conventional manner, but the color filters may be used to measure the intensity of particular colors or the relative proportion of color mixtures. For example, the red filter may be used to measure the intensity of red vegetation in an infrared image. It is also possible to measure the amount of blue and green color in the red vegetation by rotating the blue and green filters over the red vegetation and again mak-

ing light intensity readings. When the red, blue and green voltages are added together, the sum should equal one, or unity.

The line trace densitometer is one of the earliest devices used for measuring image density. It consists of a stationary light source above which is a tracking table with a hole or aperture in the center. The tracking speed of the table is variable by using different motor speeds. An image is on the table which then tracks over the light source. Image densities are transmitted into a photomultiplier tube and recorded as voltage readings on a chart.

Density "profilers" are more sophisticated versions of the line trace densitometer. They consist of a light table, an overhead television camera, and a closed circuit television monitor. The image is placed on the light table and is broadcast by the camera onto the television monitor. The density profiler projects a straight vertical white line onto the left side of the monitor and this serves to indicate those areas on the image whose densities are to be measured. All of the points lying on the line, called the "reference line", are measured. In order to measure points which are not on the line, it is necessary to move the image or the reference line.

On the right side of the monitor a second vertical white line is projected, called a "density profile line". This line represents a line trace of the actual density values of the area superimposed by the reference line and has peaks and valleys or "zigzags." The density value is represented by the horizontal distance between a point on the reference line and its corresponding point on the profile line and this distance is measured by a "micrometer line." The micrometer line is horizontal and can be adjusted to any desired length. It can be moved up, down, or sideways by using a control stick, but it is always kept in horizontal configuration. The density of a point, a corn field for example, is measured by placing one end of the micrometer line where the reference line crosses the corn field. The micrometer line is then lengthened until it touches the density profile line, and the digital readout of the line length is then recorded.

These line lengths must then be converted into density values. This is done by using a conversion graph made by measurements from a density step wedge or grey scale. The step wedge is projected onto the monitor and the micrometer readings for each step are recorded. A curve is then drawn by plotting the micrometer readings against the known density values. From this curve, it is possible to find the

density value of any point on the image as long as its micrometer value is known.

Spot and line-trace densitometric methods are outdated from the standpoint that the resulting density data are graphable by hand only and cannot be done automatically by computer without first putting the data on cards. Scanning densitometers, on the other hand, can be used in conjunction with computer systems. The scanning densitometer consists of a horizontally tracking light source surrounded by a cylinder on which an image is mounted. The cylinder is rotated at high speed while the light source traverses its length. Each point on the image is eventually viewed by the light source and its output voltage (image density) amplified by a photomultiplier tube. The voltages are then sampled by an analog-to-digital converter and stored on magnetic tape. Once in this form, the image data can be analyzed by exactly the same processes as Landsat digital tapes.

Digital Data Tapes. Multispectral scanner data are most versatile in the form of computer tapes. The Landsat I and II scanner data are prime examples of the utility of this format, as attested by the massive research and development effort to create automatic processing algorithms for theme extraction. One can purchase Landsat computer tapes from EROS Data Center either in 7 or 9 track format and 800 or 1600 bits per inch (BPI).

Software packages to accompany these tapes are available under the names of LARSYS and CMS II among others. The LARSYS processing package, prepared at Purdue University, contains several thousand computer statements. These enable the research investigator to automatically classify the contents of a scene; to ratio data from individual channels; to make radiometric, geometric and atmospheric corrections; or to composite data from non-remotely sensed sources onto the pixels recorded by Landsat.

The output from such efforts can be displayed on a color television monitor with specific colors assigned to each category, or, they can be assigned a computer print symbol and printed by a high speed printer. Examples of both output formats are given in Plate 6A and B. Usually the output from high speed printers is performed in black and white. In the example shown in Plate 6C from Colorado State University, color has been added by printing the output on a special ribbon having several colors of ink.

One of the main requirements for effective use of computer tapes, especially with Landsat data, is

the ability to locate the area of geographic interest. Remembering that there are approximately 2340 scan lines and 3240 samples per scan line, the usual technique for locating an area on the digital tape is to define the coordinates as shown in Plate 7. A specially prepared transparent overlay is placed over a 1:1,000,000 scale image represented on the tape. There are separate overlays for locating scan lines and samples. By then in-putting these coordinates into the computer, only the digital values for the area contained therein will be processed.

The main advantage of displaying small areas within the data is that scale adjustments are possible. By choosing to display only part of the data (say, every fourth line, and every fourth sample), the output TV screen can show the entire 1:1,000,000 scale image. As more and more of the data are displayed, or in other words, as the area of interest within the scene becomes smaller, larger scales can be achieved. On the LARSYS system, it is possible to display every line and every pixel for small areas and thereby achieve scales on the order of 1:24,000, the standard USGS topography scale. Plate 8A through D shows a sequence of computer processed Landsat data. The top example is at a scale of 1:1,000,000 and the bottom example is at a scale of 1:24,000. All are from the same data tape for an area near Bangkok, Thailand. The arrow in each scene points to the same spot. Obviously, the larger the scale, the more detail is visible. Each pixel in the bottom image is approximately 1.1 acre in size. The rectangular block structure is a moat around a temple compound and the temple itself is indicated by the blue and white pixels clustered together inside the moat on the right hand side. The shades of red, orange and black within the compound relate to grass vigor and standing water.

Classification Strategies. For digital processing by computer, there are two basic classification strategies. These are referred to as "supervised" and "un-supervised", depending upon whether the interpreter chooses to in-put known information or let the statistics of the data govern the analysis. There are valid arguments for both approaches.

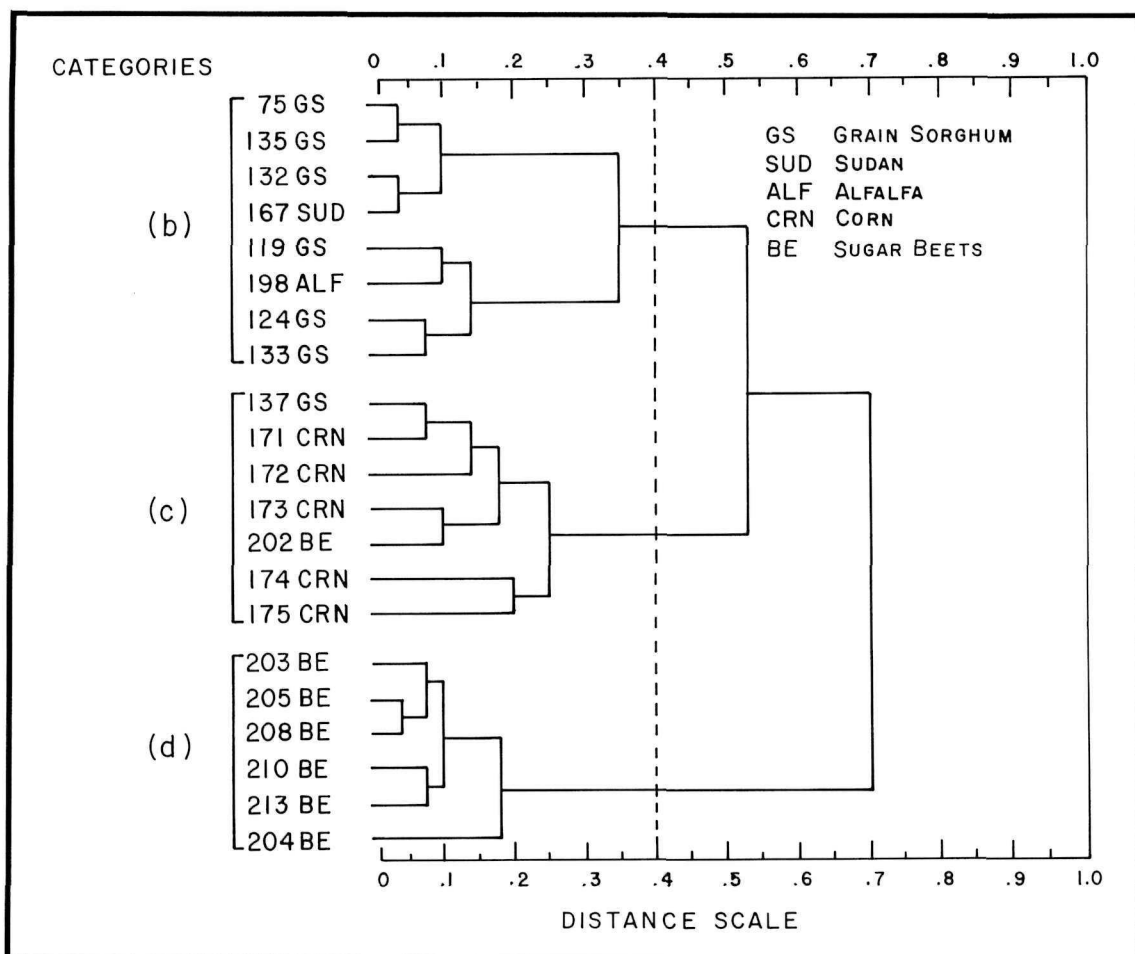
Unsupervised classification, of the type used in numerical taxonomy for species classification (Sokal and Sneath, 1963), has been adapted to image digital data to classify land uses and agricultural crops. In this strategy, the interpreter assumes no *a priori* knowledge of the items to be classified. Instead, the total population of data points is inspected for statistical relationships and clustered in similar groupings. It is then up to the interpreter to

assign names to those groupings. Clusters can be formed in either of two ways; by progressive division of the total data set, or by building groups through progressive addition (agglomeration) of data points. The divisive approach works, in practice, exactly the same as a dichotomous key. One by one, the attributes of the population are reviewed. Those elements of the population having a given attribute form one subgroup; those not having the attribute form another subgroup. All elements of the population are classified into one of the two subgroups. Each subgroup is then inspected for the presence or absence of a second, more specific attribute. The subgroup is again divided into two parts. This process continues until all attributes of interest have been used and the original data set has been divided into meaningful clusters. Obviously by using enough specific attributes, it would be possible to divide the original population into single, unique elements. An arbitrary cut-off point is therefore required of the interpreter.

The agglomerative approach, unlike the divisive, begins the grouping process by reviewing the attributes of a single individual. For example, one might create a vector of spectral responses for a given pixel of Landsat data over a one year period. Using this as a reference, a new, perhaps adjoining pixel, could be compared. If the vector signature for the second pixel is the same, or nearly so by some threshold criterion, it would be grouped with the first; if not, it would be set aside in computer memory as the first member of a second group. Continuing this process through all remaining pixels of a given area, a set of groups would be formed that would be internally homogeneous and externally different. Points not falling neatly into a major grouping can be assigned to a group calculating, among other measures, euclidean distances between those points and the centroids of the groups.

Unsupervised classification techniques have several distinct advantages:

- 1) No prior knowledge of the site is required.
- 2) Human bias is minimized.
- 3) Classes are, generally, more homogeneous and it is easier to select a class title or description after reviewing all members of a class than it is to identify a class and then have the computer search for the class number.
- 4) The techniques identify those data points in the set that are unique or residual. These points then become a focus for further inquiry. Figure 3-6, for example, shows in



3-6 Example of unsupervised computer classification of crop clusters derived from densitometry of a radar image.
Source: Schwarz and Caspell, 1968.

graphical form a series of crop clusters derived from densitometry of a radar image. At the arbitrary cut-off of $r=0.4$ (distance correlation) the groups are relatively homogeneous. In group C, however, it is apparent that one grain sorghum field and one sugar beet field had statistics easily confused with corn. These would warrant further field investigation for explanation.

All *supervised* classification algorithms require *a priori* knowledge of the terrain and the kinds of categories desired from the analysis. Using the supervised approach, a satellite or aerial photograph is examined manually and known areas or "training sets" are identified. Usually several training areas are selected for each class desired to be mapped. These sets are then given coordinate

locations and fed into the computer for data manipulation. Once the computer has been "trained" or supervised in the identification of these sets, it is then instructed to classify all other data points in the image. Clearly, in this approach, the interpreter is responsible for defining the number and identifying attributes of the classes.

Nearly all current work in Landsat digital image analysis uses supervised rather than unsupervised classification. The output from these algorithms has been discussed in the preceding section. The main attributes of supervised classification are:

- 1) Prior knowledge (usually as field data) is required for the area to be classified.
- 2) The areas chosen for the training sets may

not be completely representative of a given class description and, therefore, the final map output could be inaccurate. There is usually a category labeled as "other" for all pixels not adhering to the input constraints.

- 3) The spectral signatures obtained from the training sets are often representative only for one time and location; therefore, the training sets might need to be reidentified or rechosen for each data set and each different time period. Nevertheless, since the categories are preselected, considerable computer and interpretation time can be saved.

Computer classifications of these types may well have applications in archeology. If prehistoric camp sites or field patterns are known and can be identified by a spectral signature, they might be useful as computer training sites. It might then be possible for the computer to look for similar sites or features in the same area. These classifications would, at best, give a possible area to field check, but this alone could save a considerable amount of time and effort.

Band Ratioing. Band ratioing is a specific and growing area of interest in digital image processing. Ratioing is simply the division of one spectral band by another on a pixel-by-pixel basis to accentuate subtle differences in surface reflectances. The result is then displayed on the TV monitor as a new image. Most often the simple ratios are prepared using digital data from two channels of a single Landsat scene. More complicated ratios can be created using data from two different time periods. The most complex of all are composite ratios created by displaying three simple ratios in different colors and superimposing them on a TV screen.

For much of the ratioing work using Landsat data, a number of data corrections are necessary. Radiometric corrections are required to equalize the detector response for the six separate detectors of each band. These six detectors do not produce the same output for a given input. However, one assumes that the outputs of the detectors are linearly related for the same input. The radiometric correction consists of choosing one detector as standard and calibrating the others against it.

Atmospheric corrections are also required, especially in the case of temporal ratios where different atmospheric conditions have prevailed. Plate 9 shows examples of haze and solar corrections. A crude correction for haze can be calculated by locating areas on the image that would be expected

to have no energy return (zero volt response) such as cloud shadows. By then looking at the pixel values for those areas, the computer can adjust the observed value to zero and at the same time subtract an equivalent amount from every other pixel. This difference is assumed to be roughly equal to the atmospheric haze factor. More involved procedures have been documented (Chavez, 1975) for this correction, but their impacts on subsequent image interpretation have not been assessed.

A third type of correction, again, needed for temporal ratioing, is for solar elevation. Images obtained over several seasons, even though imaged at the same local sun time of 0930, have been illuminated with the sun at different elevations. A correction is necessary, therefore, to adjust average brightness over the entire scene. It is accomplished by multiplying pixels in the scene by a constant which is a function of sun elevation angle. The correction does not alter shadows or topographic expression from season to season, but does equalize overall image brightness. An example is given in Plate 9.

Once corrections have been performed, the pixel values from one band can be ratioed with those of another. The rationale behind the ratio then becomes the all important consideration. In the botanical sciences, two simple ratios have received most attention: the green/red ratio and the red/infrared ratio. In the first instance, it is reasoned that, as vegetal cover increases in density of leaf area, the green reflectance will increase, that is, the more bare soil is exposed to the scanner in the green channel, the darker grey it will appear. As the ground becomes covered, the tone will become lighter grey. Conversely, as vegetal cover increases, reflectance in the red channel will decline (greater absorption of red by chlorophyll). Therefore, a simple ratio of the pixel values for these two channels over, say, a cropping season, should give some estimate of leaf area index (LAI) and crop vigor.

Another, more complicated ratio, designed for interpreting vegetation biomass, is the red/infrared ratio (Rouse, et al., 1973). In this case, a so-called "vegetation index" is calculated, not for display as an image, but rather as a quantitative estimate. A new pixel parameter is created by the equation shown below:

$$\text{Vegetation Index} =$$

$$\frac{\text{Infrared Channel} - \text{Red Channel}}{\text{Infrared Channel} + \text{Red Channel}}$$

Recent attempts to locate subtle, almost in-

visible, tonal contrasts on the earth's surface have led to the creation of composite ratios. In the example shown in Plate 10, the ratio of green to red was displayed in green; the green/infrared (700-800 nm) ratio was displayed in red; and the green/infrared (800-1100 nm) ratio was displayed in blue. All were then superimposed to provide the example shown. Again, the rationale for these selections is not clear but the result, which then becomes a focus for interpretation, vividly enhances surface features that were not previously detectable in the standard color composite.

Enhanced natural color and image ratioing have had their major applications in soils and geologic mapping as well as in vegetation and crop identification. Their applications in archeology would seem to be equally broad. The techniques could be used for pinpointing exposed rock formations which ancient cultures used as quarry sites. This will be especially helpful in areas which are remote or poorly explored in a geologic sense. The location of mineral-bearing formations which were known to have been utilized by ancient cultures would be a great help as a central point from which to begin searches for local ruins or occupation sites. They could also be used to locate certain ecological areas known to be preferred by a culture. These techniques as well as the entire Landsat system could very well be the only source of initial data collection for many hard-to-access regions of the world of interest in archeology.

Appendix

Common Conversion Factors Used in Remote Sensing

| Symbol | When you know | Multiply by | To find | Symbol |
|---------------|----------------------|---------------------|----------------|---------------|
| LENGTH | | | | |
| \AA | Angstroms | 1×10^{-10} | Meters | m |
| \AA | Angstroms | 1×10^1 | Nanometers | nm |
| \AA | Angstroms | 1×10^4 | Microns | μm |
| \AA | Angstroms | 1×10^7 | Millimeters | mm |
| nm | Nanometers | 1×10^{-9} | Meters | m |
| nm | Nanometers | 1×10^{-1} | Angstroms | \AA |
| nm | Nanometers | 1×10^3 | Microns | μm |
| nm | Nanometers | 1×10^6 | Millimeters | mm |
| μm | Microns(micrometers) | 1×10^{-6} | Meters | m |
| μm | Microns(micrometers) | 1×10^{-4} | Angstroms | \AA |
| μm | Microns(micrometers) | 1×10^{-3} | Nanometers | nm |
| μm | Microns(micrometers) | 1×10^3 | Millimeters | mm |
| mm | Millimeters | 1×10^{-3} | Meters | m |
| mm | Millimeters | 1×10^{-7} | Angstroms | \AA |
| mm | Millimeters | 1×10^{-6} | Nanometers | nm |
| mm | Millimeters | 1×10^{-3} | Microns | μm |
| mm | Millimeters | .04 | Inches | in |
| cm | Centimeters | .394 | Inches | in |
| cm | Centimeters | .033 | Feet | ft |
| in | Inches | 2.54 | Centimeters | cm |
| in | Inches | .083 | Feet | ft |
| in | Inches | .027 | Yards | yd |
| m | Meters | 3.281 | Feet | ft |
| m | Meters | 1.094 | Yards | yd |
| m | Meters | 39.37 | Inches | in |
| ft | Feet | .305 | Meters | m |
| ft | Feet | .333 | Yards | yd |
| yd | Yards | .914 | Meters | m |
| nmi | Nautical Miles | 1.852 | Kilometers | km |
| nmi | Nautical Miles | 1.151 | Statute Miles | mi |
| nmi | Nautical Miles | 1852 | Meters | m |
| nmi | Nautical Miles | 6071 | Feet | ft |
| mi | Statute Miles | .868 | Nautical Miles | nmi |
| mi | Statute Miles | 1.609 | Kilometers | km |
| mi | Statute Miles | 1760 | Yards | yd |
| mi | Statute Miles | 5280 | Feet | ft |
| km | Kilometers | .54 | Nautical Miles | nmi |
| km | Kilometers | 3281 | Feet | ft |
| km | Kilometers | .621 | Statute Miles | mi |
| km | Kilometers | 1093 | Yards | yd |

| Symbol | When you know | Multiply by | To find | Symbol |
|------------------|-----------------------|-------------------------|-----------------------|------------------|
| AREA | | | | |
| a | Acres | 4840 | Square Yards | yd ² |
| a | Acres | 43560 | Square Feet | ft ² |
| a | Acres | 4047 | Square Meters | m ² |
| a | Acres | .405 | Square Hectares | ha ² |
| a | Acres | 1.563×10^{-10} | Square Statute Miles | mi ² |
| ha | Hectares | 2.471 | Acres | |
| ha | Hectares | 1.0764×10^4 | Square Feet | ft ² |
| cm ² | Square Centimeters | .155 | Square Inches | in ² |
| in ² | Square Inches | .007 | Square Feet | ft ² |
| in ² | Square Inches | 6.451 | Square Centimeters | cm ² |
| m ² | Square Meters | 10.764 | Square Feet | ft ² |
| m ² | Square Meters | 1.197 | Square Yards | yd ² |
| m ² | Square Meters | 1550 | Square Inches | in ² |
| ft ² | Square Feet | 144 | Square Inches | in ² |
| ft ² | Square Feet | .111 | Square Yards | yd ² |
| ft ² | Square Feet | .093 | Square Meters | m ² |
| yd ² | Square Yards | 1296 | Square Inches | in ² |
| yd ² | Square Yards | 9 | Square Feet | ft ² |
| yd ² | Square Yards | .836 | Square Meters | m ² |
| mi ² | Square Statute Miles | 640 | Acres | |
| mi ² | Square Statute Miles | 2.590 | Square Kilometers | km ² |
| mi ² | Square Statute Miles | .753 | Square Nautical Miles | nmi ² |
| nmi ² | Square Nautical Miles | 3.40 | Square Kilometers | km ² |
| nmi ² | Square Nautical Miles | 1.324 | Square Statute Miles | mi ² |
| km ² | Square Kilometers | .386 | Square Statute Miles | mi ² |
| km ² | Square Kilometers | .292 | Square Nautical Miles | nmi ² |
| VELOCITY | | | | |
| ft/sec | Feet/Second | .305 | Meters/Second | m/sec |
| ft/sec | Feet/Second | .682 | Statute Miles/Hour | mi/hr |
| ft/sec | Feet/Second | .593 | Nautical Miles/Hour | knots |
| m/sec | Meters/Second | 3.281 | Feet/Second | ft/sec |
| m/sec | Meters/Second | 2.237 | Statute Miles/Hour | mi/hr |
| m/sec | Meters/Second | 1.946 | Nautical Miles/Hour | knots |
| mi/hr | Statute Miles/Hour | 1.609 | Kilometers/Hour | km/hr |
| mi/hr | Statute Miles/Hour | .868 | Nautical Miles/Hour | knots |
| knots | Nautical Miles/Hour | 1.852 | Kilometers/Hour | km/hr |
| knots | Nautical Miles/Hour | 1.151 | Statute Miles/Hour | mi/hr |
| km/hr | Kilometers/Hour | .621 | Statute Miles/Hour | mi/hr |
| km/hr | Kilometers/Hour | .540 | Nautical Miles/Hour | knots |

Selected References

- Batuscheck, C. P. "Ground Temperature and Thermal Infrared," *Photogrammetric Engineering*, XXXVI, No. 10 (1970), 1064-1072.
- Bevan, Bruce W. *Aerial Photography for the Archaeologist—A Report From the Museum Applied Science Center for Archaeology*. Philadelphia: the University Museum, University of Pennsylvania, 1975.
- Breiner, S. *Applications Manual for Portable Magnetometers*, Sunnyvale, California: Geometrics, 1973.
- Bryan, M. L. *Radar Remote Sensing for Geosciences: An Annotated and Tutorial Bibliography*, Washington: Environmental Research Institute of Michigan for the National Science Foundation, 1973.
- Chase, M. E. "Airborne Remote Sensing for Groundwater Studies in Prairie Environment," *Canadian Journal of Earth Sciences*, VI, No. 4, Part 1 (1969), 737-741.
- Chavez, Jr., P. S. "Atmospheric, Solar, and MTF Corrections for ERTS Digital Imagery," *Proceedings of the Fall Convention—American Society of Photogrammetry*, Phoenix, 1975, 69-70.
- Committee on Remote Sensing for Agricultural Purposes (eds.). *Remote Sensing with Special Reference to Agriculture and Forestry*. Washington: National Academy of Sciences, 1970.
- Cronin, J. F.; Rooney, T. P.; Williams, Jr., R. S.; Molineaux, C. E., and Blamptis, E. E. *Ultraviolet Radiation and the Terrestrial Surface*. Special Report No. 83, AF CRL-68-0572, Bedford, Massachusetts: Air Force Cambridge Research Laboratories, 1968.
- Eagleton, Joe R.; Pogge, Ernest C.; and Moore, Richard K. *Detection of Soil Moisture and Snow Characteristics from Skylab*, University of Kansas, Lawrence, Kansas: Atmospheric Science Laboratory, Space Technology Center, Center for Research, Inc., 1975.
- Edgerton, A. D. and Trexler, D. T. "Oceanographic Applications of Remote Sensing With Passive Microwave Techniques," in Holz, Robert K. (ed.), *The Surveillant Science—Remote Sensing of the Environment*. Boston: Houghton Mifflin Publishing Co., 1973.
- Estes, John E., and Senger, Leslie W. (eds.). *Remote Sensing—Techniques for Environmental Analysis*, Santa Barbara: Hamilton Publishing Company, 1974.
- Fredan, Stanley C.; Mercanti, Enrico P.; and Becker, Margaret A. (eds.). *Symposium on Significant Results Obtained from Earth Resources Technology Satellite—I*, Vol. I, Technical Presentations, Sections A and B, Washington: National Aeronautics and Space Administration, 1973.
- General Electric—Space Division. *Earth Resources Technology Satellite Reference Manual*, General Electric Co.
- Hardy, Norman E. *Interpretation of Side Looking Airborne Radar Vegetation Patterns: Yellowstone National Park*. Thesis, Department of Geography, University of Kansas, Lawrence, Kansas, 1973.
- Holter, M. P. "Infrared and Multispectral Remote Sensing," *Proceedings of NATO AGARD XCVII EPP Technical Meeting*, Colorado Springs, 1971.
- Holz, Robert K. (ed.). *The Surveillant Science—Remote Sensing of the Environment*. Boston: Houghton Mifflin Publishing Co., 1973.
- Johnson, Philip L. (ed.). *Remote Sensing in Ecology*, Athens, Georgia: University of Georgia Press, 1969.
- Kennedy, J. M.; Edgerton, A. T.; and Sakamoto, Mandl. *Passive Microwave Measurements of Snow and Soil*, Report Prepared for Geography Branch, Office of Naval Research, Washington, 1966.
- Kruckman, Lawrence. "Remote Sensing and Archeology: A Preliminary Bibliography," in *RSEMS*, Newsletter of the Remote Sensing Committee of the Association of American Geographers, Vol. 3, No. 2, 1976.
- Lewis, A. J.; MacDonald, H. C.; and Simonett, D. S. "Detection of Linear Cultural Features with Multipolarized Radar Imagery," in *Proceedings of the Sixth International Symposium on Remote Sensing of the Environment*, Willow Run Laboratories of the Institute of Science and Technology, University of Michigan, Ann Arbor, Michigan, 1969.
- Lewis, A. J., and Waite, W. P. "Radar Shadow Frequency," *Photogrammetric Engineering*, XXXVIII, No. 2 (1973), 189-196.
- Lyons, Thomas R., and Ebert, James I. "Archaeological Analysis of Imagery of Chaco Canyon Region, New Mexico," in *ERTS-I: A New Window on Our Planet*, USGS Professional Paper 929, 304-306, 1976.
- MacDonald, H. C., and Waite, W. P. "Optimum Radar Depression Angles for Geological Analysis." *Technical Report 177-9, CRES*, University of Kansas, Lawrence, Kansas, 1970.
- Morain, S. A. "Phenology and Remote Sensing," in Lieth, Helmut (ed.) *Phenology and Seasonality Modeling, Ecological Studies, Analysis and Synthesis*, Vol. 8, New York: Springer-Verlag New York Inc., 1974.

- Morain, S. A. and Campbell, J. B. "Radar Theory Applied to Reconnaissance Soil Surveys," in *Proceedings of the Soil Science Society of America*, XXXVIII, No. 5, Madison, Wisconsin, 1974.
- Morain, S. A. and Simonett, D. S. "Vegetation Analysis with Radar Imagery," *Proceedings of the 4th Symposium on Remote Sensing of the Environment*, University of Michigan, Ann Arbor, Michigan, 1965.
- Moore, R. K. "Ground Echo," in Skolnik, M. I. (ed.), *Radar Handbook*, New York: McGraw-Hill, 1970.
- National Aeronautics and Space Administration. *Earth Resources Technology Satellite Data Users Handbook*, Greenbelt, Maryland: Goddard Spaceflight Center, 1972.
- Nunnally, Nelson R. *Introduction to Remote Sensing—the Physics of Electromagnetic Radiation*, Prepared for the Association of American Geographers Commission on Geographic Applications. Johnson City, Tennessee: East Tennessee State University, 1969.
- Offield, Terry W. "Line-Grating Diffraction in Image Analysis: Enhanced Detection of Linear Structures in ERTS Images, Colorado Front Range," *Modern Geology*, V (1975), 101-107.
- Peterson, R. M.; Cochrane, G. R.; Morain, S. A.; and Simonett, D. S. "A Multisensor Study of Plant Communities at Horsefly Mountain, Oregon," in Johnson, Philip L. (ed.). *Remote Sensing in Ecology*, Athens, Georgia: University of Georgia Press, 1969.
- Proceedings of the International Symposia on Remote Sensing of the Environment*, Environmental Research Institute of Michigan, 1962-1975.
- Reeves, Robert G., (ed.). *Manual of Remote Sensing, Volumes I and II*. Falls Church, Virginia: American Society of Photogrammetry, 1975.
- Rouse, J. W.; Haas, R. H.; Schell, J. A.; and Deering, D. W. "Monitoring Vegetation Systems in the Great Plains with ERTS," in Fredan, Stanley C.; Mercanti, Enrico P.; and Becker, Margaret A. (eds.). *Symposium on Significant Results Obtained from Earth Resources Technology Satellite-1*, Vol. 1 Technical Presentations, Section A, Washington: National Aeronautics and Space Administration, (1973), 309-317.
- Rudd, Robert D. *Remote Sensing—A Better View*. Belmont, California: Duxbury Press, 1974.
- Sabatini, R. R.; Rabchevsky, G. A.; and Sissala, J. E. *Nimbus Earth Resources Observations*, Technical Report #2, Concord, Massachusetts: Allied Research Associates, 1971.
- Schaber, G. G., and Gumerman, G. J. "Infrared Scanning Images: An Archaeological Application," *Science*, CLXIV, No. 3880 (1969), 712-713.
- Scherz, James P. and Stevens, Alan R. *An Introduction to Remote Sensing for Environmental Monitoring*, University of Wisconsin: Remote Sensing Program, Institute for Environmental Studies, 1970.
- Schwarz, David E. and Caspell, Fred. "The Use of Radar in the Discrimination and Identification of Agricultural Land Use," in *Proceedings of the Fifth International Symposium on Remote Sensing of the Environment*, Willow Run Laboratories of the Institute of Science and Technology, University of Michigan, Ann Arbor, Michigan, (1968), 233-247.
- Shahrokhi, F. (ed.). *Remote Sensing of Earth Resources, Volumes I to IV*. Tullahoma, Tennessee: University of Tennessee Space Institute, 1972-1975.
- Sokal, R. A., and Sneath, P. H. A. *Numerical Taxonomy*, San Francisco: W. H. Freeman, 1963.
- Spirakis, Charles S., and Condit, Christopher O. *Preliminary Report on the Use of Landsat I (ERTS-I) Reflectance Data in Locating Alteration Zones Associated with Uranium Mineralization Near Cameron, Arizona*. Unpublished Open-File Report, Denver: U.S. Geological Survey, 1975.
- Stringham, J. A. and Williams, R. S., Jr. "Applications of Reconnaissance Concepts to Mapping Problems," in *Proceedings of the Geodetic and Research and Development Symposium*, Seventh Department of Defense Geodetic—Cartographic Target Materials Conference, Cameron Station, Virginia, 1970.
- Technology Reports Center
Handbook of Remote Sensing Techniques, Technology Reports Center, Kent, United Kingdom, 1973.
- Wenderoth, Sondra; Yost, Edward; Kalia, Rajender; and Anderson, Robert. *Multispectral Photography for Earth Resources*. Huntington, New York: West Hills Printing Company, 1974.
- Wermund, E. G. "Remote Sensors for Hydrologic Prospecting in Arid Terrains," *IEEE Transactions on Geoscience Electronics*, GE-9, No. 3 (1971), 120-130.



As the Nation's principal conservation agency, the Department of the Interior has responsibility for most of our nationally owned public lands and natural resources. This includes fostering the wisest use of our land and water resources, protecting our fish and wildlife, preserving the environmental and cultural values of our national parks and historical places, and providing for the enjoyment of life through outdoor recreation. The Department assesses our energy and mineral resources and works to assure that their development is in the best interests of all our people. The Department also has a major responsibility for American Indian reservation communities and for people who live in Island Territories under U.S. administration.

